KU KDM 2016
Konferencja Użytkowników Komputerów Dużej Mocy
Zakopane, 16-18 marca 2016 r.

HYBRID ON-LINE MEASUREMENT AIDED EVALUATION OF SAFE OVERHEAD POWER LINE CLEARANCE

(EKSPERYMENTALNIE WSPOMAGANE OSZACOWANIE
BEZPIECZNEJ SKRAJNI LINII ENERGETYCZNYCH WYSOKICH NAPIĘĆ)

Sławomir Milewski, Witod Cecot, Janusz Orkisz

Institute for Computational Civil Engineering
Cracow University of Technology

1. INTRODUCTION

1. INTRODUCTION

1.1 Research subject

Today talk is about energy **transmission** by overhead power lines.
Everybody needs this energy. Are there any **obstacles** in energy transmission?

troubles	- **limited** level of energy supply
reality	- **ageing** (40 years) infrastructure
	- **only two** allowed transmission **safety** thresholds: summer (high temperature) and winter (ice)
change proposed	- **D**ynamic **M**anagement of **S**afe **P**ower **T**ransmission using innovative on-line (SDZP) measurements
effect	- estimated gain DMSET < 15% **graphene** 100% ÷ 200%
consortium	- Universities 5, Polish Academy of Sciences, Companies 2, Network operators 3
sponsorship	- **E**cologic **C**oncepts **G**enerator (GEKON)

1. INTRODUCTION

GEKON Project:

Ecologic Concepts Generator – National Foundation

SDZP Project – consortium

Dynamic management of transmission abilities of overhead power transmission lines using **innovative measurement** techniques

This research

Measurements aided **numerical analysis** of large 3D displacements of extensible cables in overhead power **transmission lines**

CONTENTS

1. INTRODUCTION

1.2 Problem characteristics

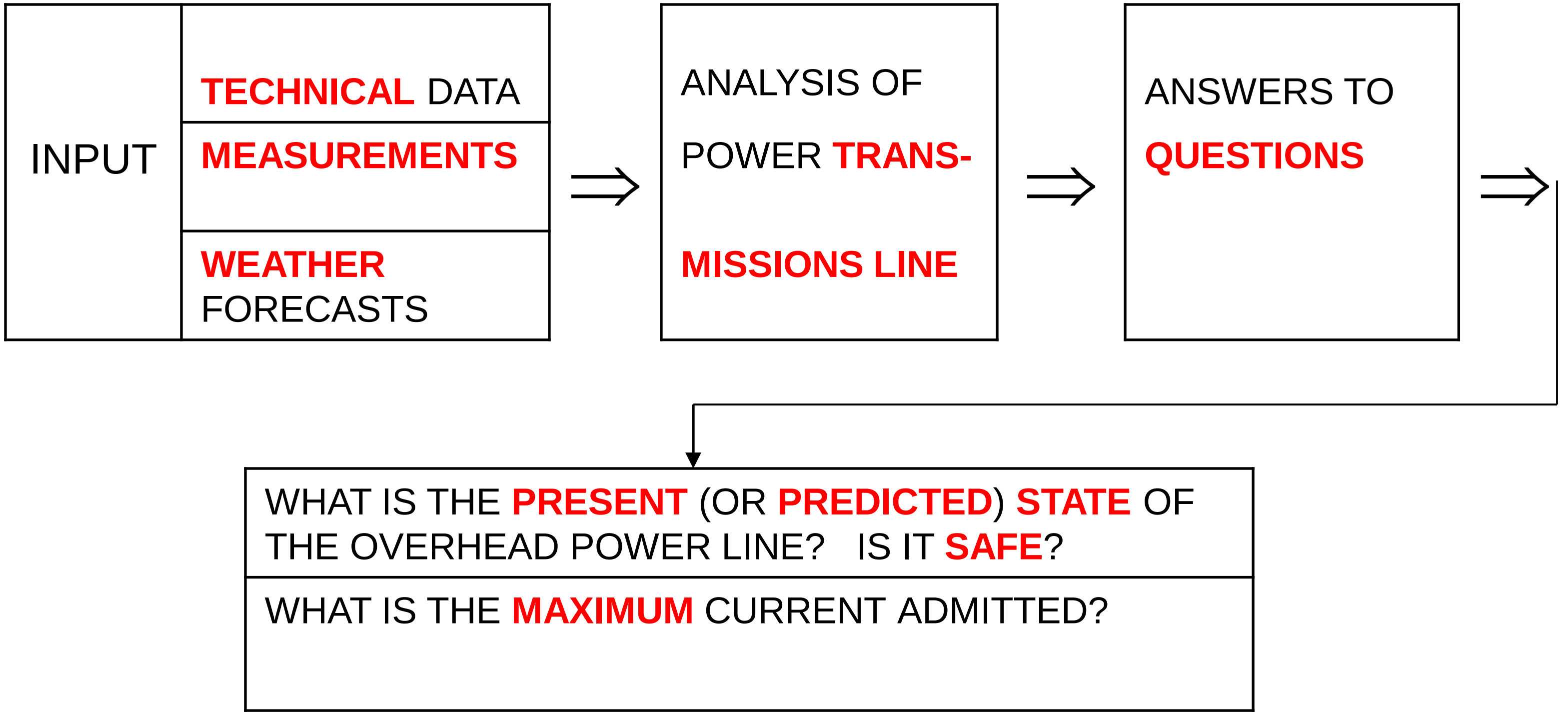

1.3 Main objectives of the research program

SDZP project

- Provide ways and tools for the **optimal** dynamic **management** of **safe** overhead power transmission

Our research

- Using innovative **on-line measurements** develop reliable and efficient tools of **3D on-line analysis** of conductors behaviour in overhead power **transmission lines**.
- Examine various **mechanical** models, their **mathematical formulations** (strong, weak, hybrid mixed), and discrete solution methods (FEM, MFDM, PBA) in order to **find** the **best** solution approach.

1.4 Categories of engineering tasks involved

I. Evaluation of the **actual**, and the **maximum current safety** of overhead power transmission lines based on technical data, and all **on-line measurements**

II. **Prediction** of overhead power transmission lines behaviour based on technical data and weather forecast (6-72 h only) while **on-line data** are **not available**

III. **Verification** of weather forecast **data** against measured on-line data, and **evaluation of prediction quality** of overhead power transmission lines behaviour

1.5 Types of general mathematical formulations of i , ii , iii problems

A) – **b.v. problem**
measured cable **inclination** and **rotation angles** are **not** taken into account

B) – nonlinear constrained **optimization** problem
all available data are considered **including measured** cable **inclination** and **rotation** angles

Mutual relation of tasks and types of problems

TASK	I	II	III
FORMULATION TYPE	B	A	A, B

2. FORMULATION OF MECHANICAL AND MATHEMATICAL MODELS OF 3D CABLE DISPLACEMENTS

2.1 Solution approach **strategy**

Special care about:

- assumptions made for **modeling** cables behaviour in a way possibly **close** to **real conductors** condition
- **high reliability** of results obtained due to
  - use of several **different** solution **approaches**
  - solution **stability**
  - **comparison** of our results with other sources of information
  - a-posteriori **error analysis**
- solution efficiency
  (**low** computational **time**, and **high** solution **convergence** rate)

2.2 On reliability of results obtained

Comparison and checking results obtained from various models

- 3 **models** 1D (inextensible and extensible), 2D, 3D
- 3 mathematical **formulations**
  - 1 **strong** (non-linear PDE)
  - 2 **weak** (variational principle)
    - **global**
    - hybrid **mixed** global-local (**MLPG-5**)
- 2 discretization **methods**
  - **FEM**
  - **MFDM** (Meshless Finite Difference Method)
- **various** approximation **orders** (1-6)
- 3 **methods** of **non-linear** analysis
  (simple iterations, Newton-Raphson, relaxation)
- 3 **independent** computer **codes** (2 own + 1 commercial)
- **a-posteriori error** analysis
- large **variety** of numerical **tests**

REFERENCES

1. Y. Huang and W. Lan. Static analysis of cable structure. Applied Mathematics and Mechanics, 27:1425–1430, 2006.
2. J. Orkisz. Finite difference method (Part III). Handbook of computational solid mechanics. Springer-Verlag, 1998.
3. W. Karmowski and J. Orkisz. A physically based method of enhancement of experimental data - concepts, formulation and application to identification of residual stresses. Proc IUTAM symp on inverse problems in eng mech, Tokyo, 1:61–70, 1993.
4. Huu-Tai Thai and Seung-Eock Kim. Nonlinear static and dynamic analysis of cable structures. Finite Elements in Analysis and Design, 47(3):237 – 246, 2011.
5. W. Cecot, S. Milewski, J. Orkisz, Measurement aided computation of extensible cable deflections, Proceedings of the 21st International Conference on Computer Methods in Mechanics, pp.215-216.

2.3 Basic assumptions for modeling of overhead power line cables

- $0 < EA < \infty$ - extensibility, no compression ($\varepsilon > 0$)
- $EI = 0$ - no resistance to bending ($M = 0$)
- thermoelastic constitutive relation $\sigma = E(\varepsilon - \alpha\Delta T) > 0$
- large displacements in 3D
- small strains
- distributed (self-weight, frost, 'wind') and concentrated loading
- elastic supporting structures with suspension insulators

2.4 Data

(i) Live (time dependent) parameters:

- T^E, T (temperature, measured or computed)
- p (wind pressure determined on the basis of its direction and velocity)
- q (distributed loading due to ice and frost - magnitude possible to be determined indirecly)
- ω^E, γ^E (cable inclination angles measured at selected places)
- concentrated forces

(ii) Parameters determined by in-situ measurements

- T_0 (initial temperature)
- ξ_0 (position of the sensor)
- L (unloaded cable length - determined indirectly)
- $a_1, \ldots, a_6$ (support coordinates)
- $\omega_0^E(T_0^E), \gamma_0^E(T_0^E), s_0^E(T_0^E), \omega_1^E(T_1^E), \gamma_1^E(T_0^E), s_1^E(T_1^E), \ldots$ (angles and sags for various temperatures for model validation)

2.4 Data continued

(iii) Material parameters:

- μ - self-weight (dead load)
- A - cable cross section area (effective)
- E - cable Young's modulus (effective)
- α - cable thermal expansion coefficient
- β - viscous parameter
- L_i, Q_i - insulator parameters
- K_1, K_2 - support stiffness matrices

(iv) Measurement accuracy:

- e_T (of temperature)
- $e_{\omega,\gamma}$ (of angles)

2.5 Boundary value problem type A - strong formulation

Find displacement components (in total Lagrangian description):

$u_1(X,t), u_2(X,t), u_3(X,t), \qquad X \in [0,L], \qquad L = L(\beta,t)$

$$
\begin{cases}
\rho \dfrac{\partial^2 u_i}{\partial t^2} - F_i' = p_i & \textbf{linear momentum} \\
F_i = AE\dfrac{\varepsilon - \alpha \triangle T}{\varepsilon + 1}(\delta_{1i} + u_i') & \textbf{constitutive relation} \\
\varepsilon = \sqrt{(1+u_1')^2 + (u_2')^2 + (u_3')^2} - 1 & \textbf{strain definition} \\
\boldsymbol{F} + \boldsymbol{K}^s(\boldsymbol{u} - \hat{\boldsymbol{u}}) = 0 \ \text{(elastic supports)} & \textbf{b.c. for } X = 0, L \\
+initial \ \ conditions &
\end{cases}
$$

$i = 1, 2, 3$
$L - unloaded \ cable \ length$
$F_i - axial \ force \ components$
$\boldsymbol{K}^s - elastic \ support \ stiffness \ matrix$
$\hat{u} - unloaded \ support \ position$

deflection curve $\gamma : \begin{cases} x = X + u_1(X) \\ y = u_2(X) \\ z = u_3(X) \end{cases}$

2.6 Boundary value problem type A - weak formulation

$\boldsymbol{u} \in H^1[0, L]$

$$\int_0^L \rho \boldsymbol{v} \cdot \ddot{\mathbf{u}} + \int_0^L \boldsymbol{v}' \cdot \boldsymbol{F} \; \mathrm{d}X - \int_0^L \boldsymbol{v} \cdot \boldsymbol{p} \; \mathrm{d}X + \sum_{k=1}^{2} \boldsymbol{v}_k^T \boldsymbol{K}_k^{(s)} \left(\boldsymbol{u}_k - \hat{\boldsymbol{u}}_k \right) = 0$$

$\forall \boldsymbol{v} \in H_0^1[0, L]$

Newton-Raphson linearization for static case $\boldsymbol{u}^{(n+1)} = \boldsymbol{u}^{(n)} + \psi$

$$\int_0^L (\boldsymbol{v}')^T \frac{\partial \boldsymbol{F}}{\partial \boldsymbol{u}'} \psi' \; \mathrm{d}X - \int_0^L \boldsymbol{v}^T \frac{\partial \boldsymbol{p}}{\partial \boldsymbol{u}'} \psi' \; \mathrm{d}X +$$

$$+ \int_0^L \boldsymbol{v}' \cdot \boldsymbol{F} \; \mathrm{d}X - \int_0^L \boldsymbol{v} \cdot \boldsymbol{p} \; \mathrm{d}X + \sum_{k=1}^{2} \boldsymbol{v}_k^T \boldsymbol{K}_k^{(s)} \left(\boldsymbol{u}_k - \hat{\boldsymbol{u}}_k \right) = 0$$

$\forall \boldsymbol{v} \in H_0^1[0, L]$

2.7 Exact analytical 3D solution – **verification** of numerical model

$$p_1 = 0; \;\; p_2 = \mu = const, \;\; p_3 = const, \;\; u_1(0) = u_2(0) = u_3(0) = 0$$

$$u_1 = \frac{Ct}{p_0} \log\left(\frac{p_0 X + D + \sqrt{C^2 + (p_0 X + D)^2}}{D + \sqrt{C^2 + D^2}}\right) + \left(\frac{C}{AE} - 1\right) X$$

$$u_2 = \frac{p_2 t}{p_0^2}\left(\sqrt{C^2 + (p_0 X + D)^2} - \sqrt{C^2 + D^2}\right) + \frac{p_0 X + 2D}{2AEp_0} p_2 X$$

$$u_3 = \frac{p_3 t}{p_0^2}\left(\sqrt{C^2 + (p_0 X + D)^2} - \sqrt{C^2 + D^2}\right) + \frac{p_0 X + 2D}{2AEp_0} p_3 X$$

$$p_0 = \sqrt{p_2^2 + p_3^2}.$$

C & D are constants that may be found from two boundary conditions $u_1(L) = c, \; \sqrt{u_2^2(L) + u_3^2(L)} = d.$

2.7 continued

Exact analytical 3D solution – **verification** of numerical model

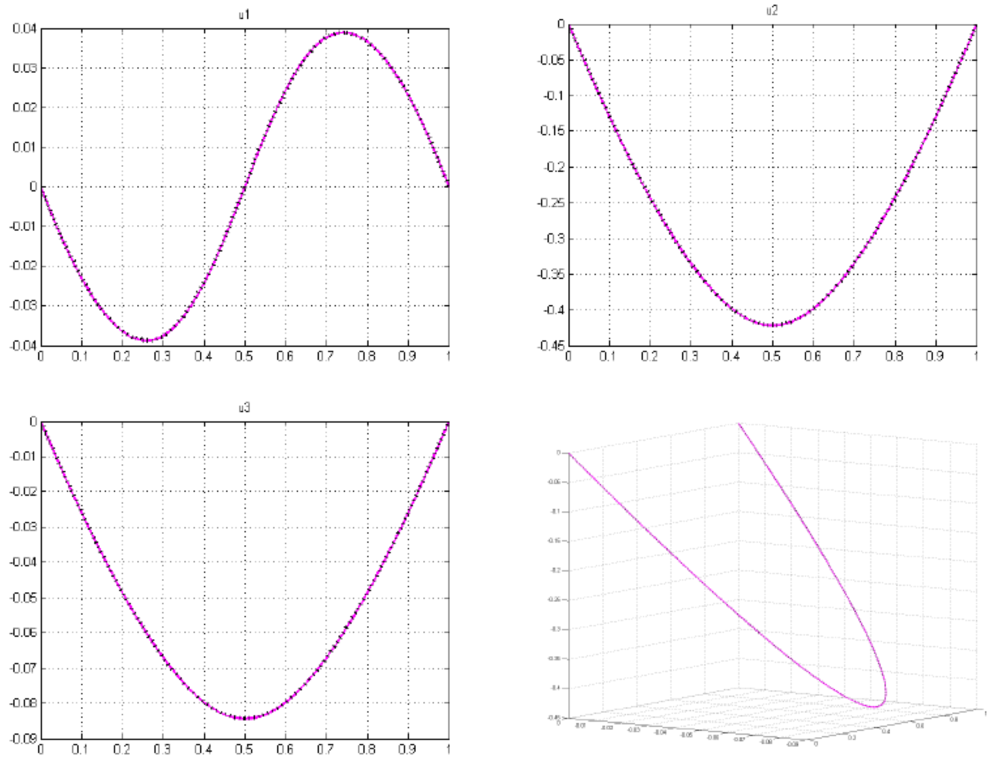

- Comparison of numerical (continuous lines) and closed form (dotted lines) solutions. The error may be aribtrarily small.

2.8 FEM approximation with Legendre polynomials

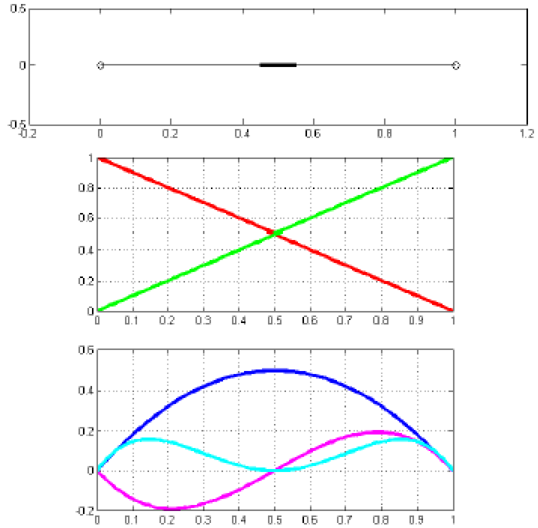

Error convergence (for u and for u') vs. time for p=1,2,...,6

and a typical exemplary problem

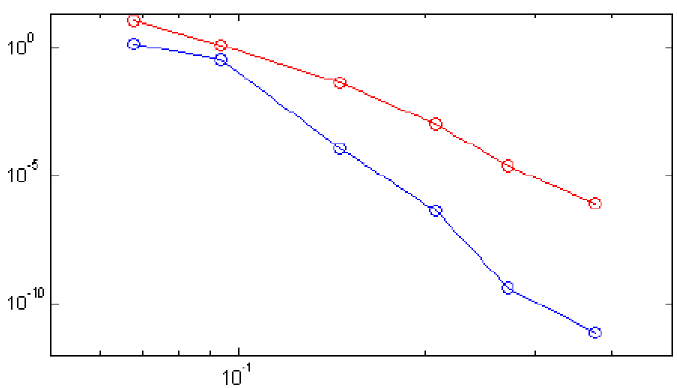

2.9 FEM approximation – optimal discretization

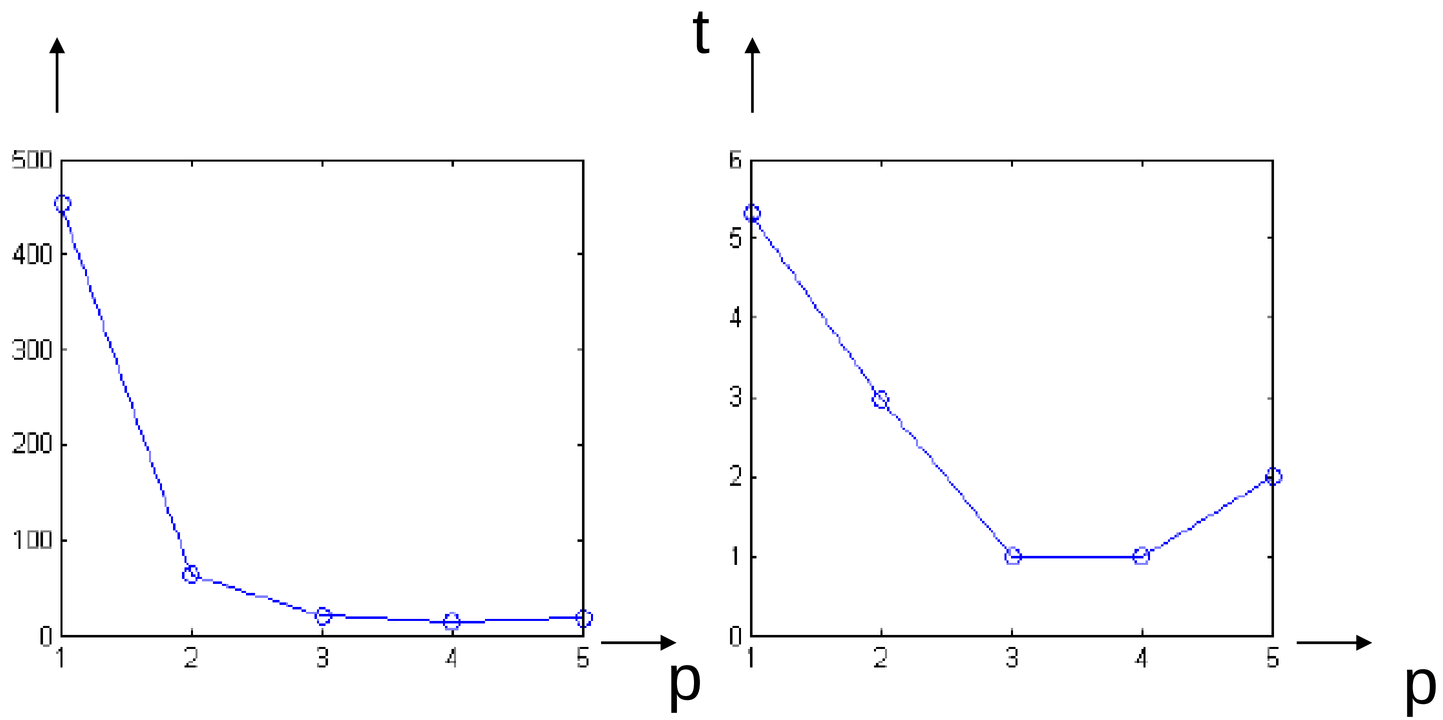

- Number of degrees of freedom and time of computation (as a multiple of the shortest time) for various orders of approximation (p=1,2,…,5).
    - Optimal discretization: 2-3 element of order 3-4 (20-40 dof).

2.10 Meshless Finite Difference Method (MFDM) solution approach

Moving **W**eighted **L**east **S**quares (MWLS) approximation

- **low order** (p = 1,2)

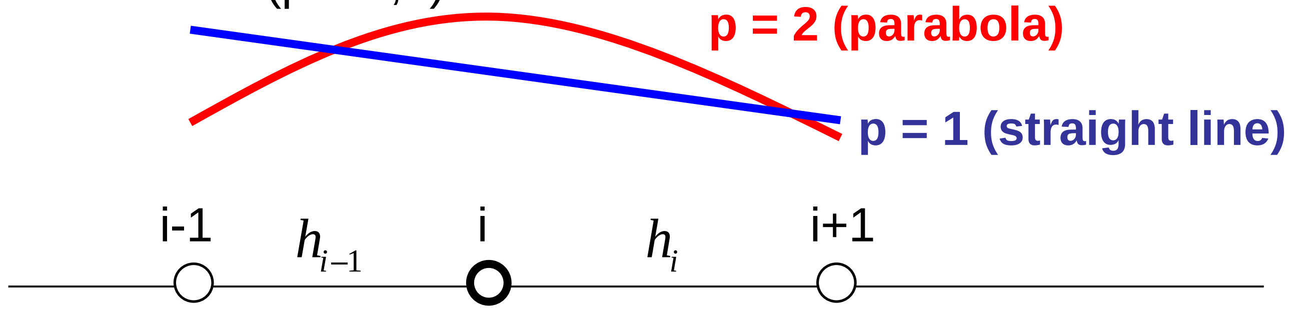

$$u_i' \approx Lu_i = a_{i-1}u_{i-1} + a_i u_i + a_{i+1}u_{i+1} \quad , \quad a_{i-1}, a_i, a_{i+1} \in \Re$$

- **higher order** (p > 2)

(i) MFD stars using increased number of nodes

(ii) correction terms for low order operator

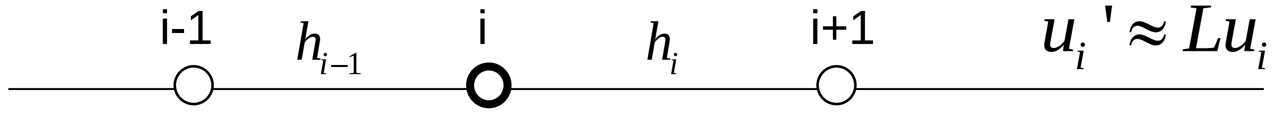

$$u_i' \approx Lu_i + \Delta_i\left(u_i^{iii}, u_i^{iv}\right)$$

2.11 Meshless Local Petrov-Galerkin (MLPG-5) formulation of b.v. problem

Test function: v = 1 -> v' = 0

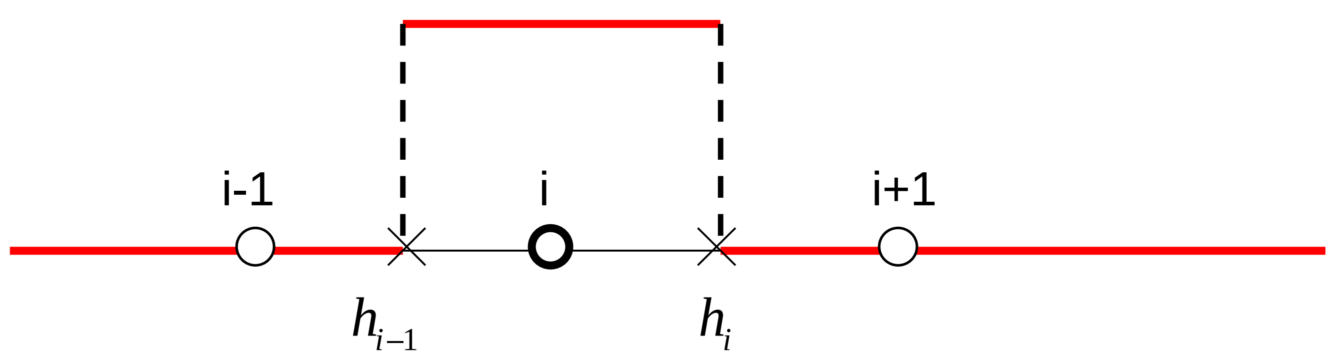

$$-\int_{x_{0(k)}}^{x_{1(k)}} \Delta p_{i,j} \frac{\partial \psi_j}{\partial X} dX_{(k)} - \left(\Delta F_{i,j}\left(x_{1_{(k)}}\right) \frac{d\psi_j}{dX}\left(x_{1_{(k)}}\right) - \Delta F_{i,j}\left(x_{0_{(k)}}\right) \frac{d\psi_j}{dX}\left(x_{0_{(k)}}\right) \right) +$$

$$-\int_{x_{0(k)}}^{x_{1(k)}} p_i dX_{(k)} = 0 \quad , \quad i, j = 1,2,3 \quad , \quad \forall_{k=2,\dots,n-1}$$

Notice: **SAE** are of **similar** type here as these for the **FEM** and **MFDM** (weak formulation).
However, in the stiffness matrix **K** one **integral disappears**. Moreover, new boundary terms emerge in the endpoints of the integration element.

3. MODELING OF SUSPENSION INSULATORS continued

Insulator suspension of length l and weight Q

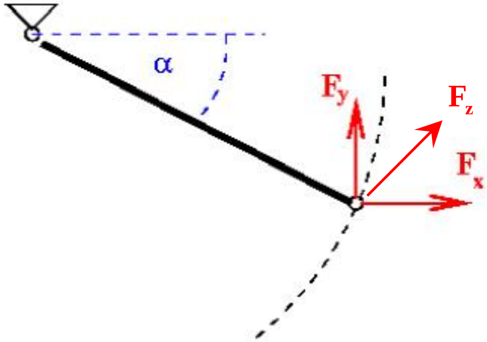

Insulator modeled as a rotating rigid body

3. MODELING OF SUSPENSION INSULATORS

$$\mathrm{tg}\alpha = \frac{\frac{1}{2}Q - F_y}{F_x} \qquad \Rightarrow \qquad \begin{cases} u_1 = x_0 + l\cos\alpha - X \\ u_2 = y_0 + l\sin\alpha \end{cases}$$

Such a condition is updated at each NR step

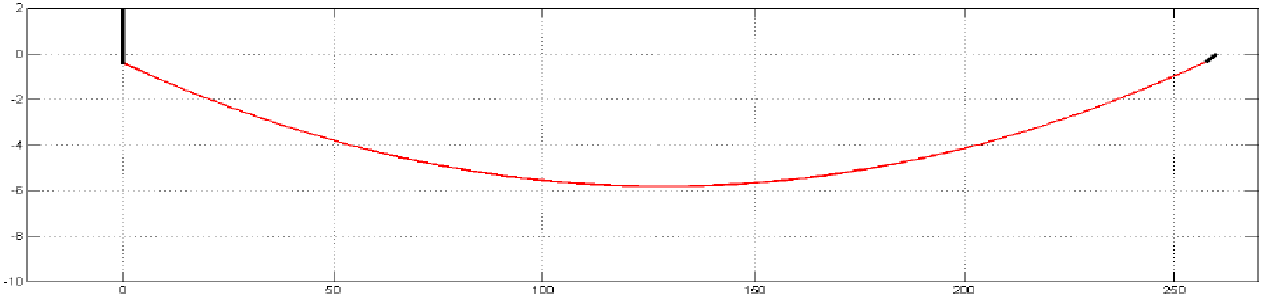

Numerically determined deflection of a cable with insulator suspension

Another possibile modeling of insulator

- use the same equations as for the cable but assume larger self-weight
- approximate insulator displacements by only 1 finite element with linear shape functions

4 NUMERICAL ANALYSIS – METHODS AND TESTS USED FOR THEORETICAL SOLUTION APPROACH

4.1 Objectives of numerical tests done

Comparison of:

(i) various **formulations** of b.v. problem (strong, weak, hybrid mixed)

(ii) various discrete solution **methods** (FEM, variational MFDM, MLPG-5 MFDM)

(iii) various types and **orders** of **approximation**

(iv) results obtained from **different** computer **codes**

(v) various types of **loading** (temperature, distributed loads and concentrated forces)

Each time considered were: solution **precision** and **convergence**, **computational** time.

Moreover the influence of

- elastic **supporting structures**
- different **phases**, ...
- number of **spans** considered

on **cable deformation** was analysed.

4.2 TEST DATA #1 (3D), from

A new deformable catenary element for the analysis of cable net structures,
A. Andreu,L. Gil, P. Roca, Comp & Struct, 2006

$E = 1.31045$ GPa, $A = 5.48\text{e-}4\ m^2$
$L = 312.73$ m, $L_c = 304.8$ m
$\alpha = 20\text{e-}6$ 1/K, $\Delta T = 3$ K, $\mu = 5$ N/m, $H_1 = H_2$
$q_x = q_y = q_z = -20\text{e-}3$ N/m and/or $P_x = P_y = P_z = -35.5979$ N

TEST DATA #2 (**ENERGOPROJEKT**, 2D): line *AFL-6 120 mm²*

$E = 75.188$ GPa, $A = 1.435\text{e-}4\ m^2$
$L = 260$ m + 280 m + 300 m, $L_c = 260.71$ m
$\alpha = 1.87\text{e-}6$ 1/K, $\Delta T = 0$ K ÷ 80 K, $\mu = 4.95$ N/m, $H_1 = H_2$
$q_x = q_y = 0$ N/m and $P_x = P_y = 0$ N

Additional data assumed

number of load **increments**	M=5 ÷100
number of **nodes** in a span	21 ÷ 105
numerical error **tolerance**	1e -16
starting configuration	catanary curve

4.3 Analysis of **benchmark** problems

TEST DATA #1 - distributed loads

Comparison of **methods** 1. FEM, 2.MFDM, 3. MLPG-5/MFDM

21 nodes, computational time 1: 2s, 2: 4s, 3: 10s

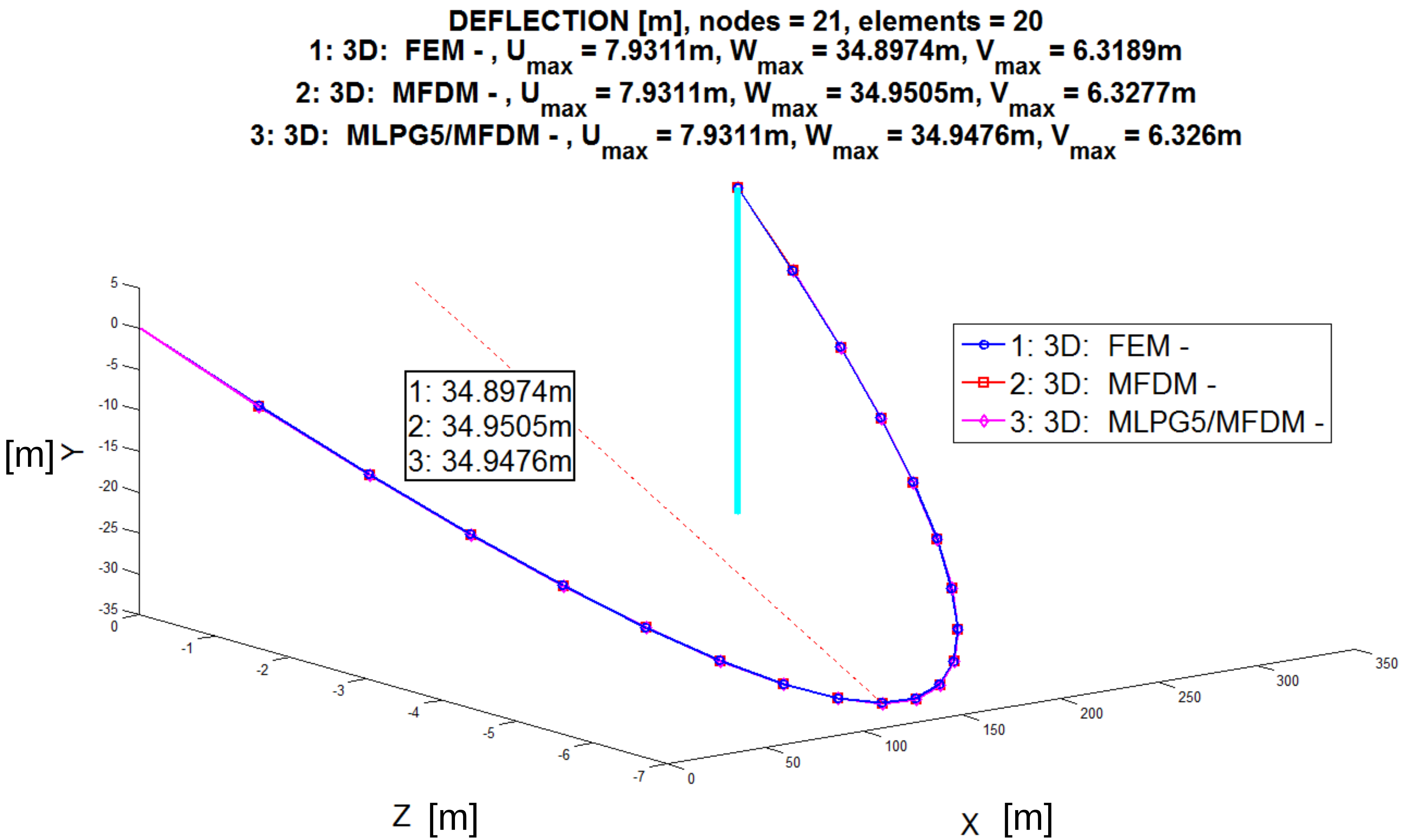

TEST DATA #1 concentrated forces

Comparison of methods 1. FEM , 2. MFDM , 3. MLPG-5/MFDM

21 nodes, computational time, 1: 1s, 2: 2s, 3: 5s

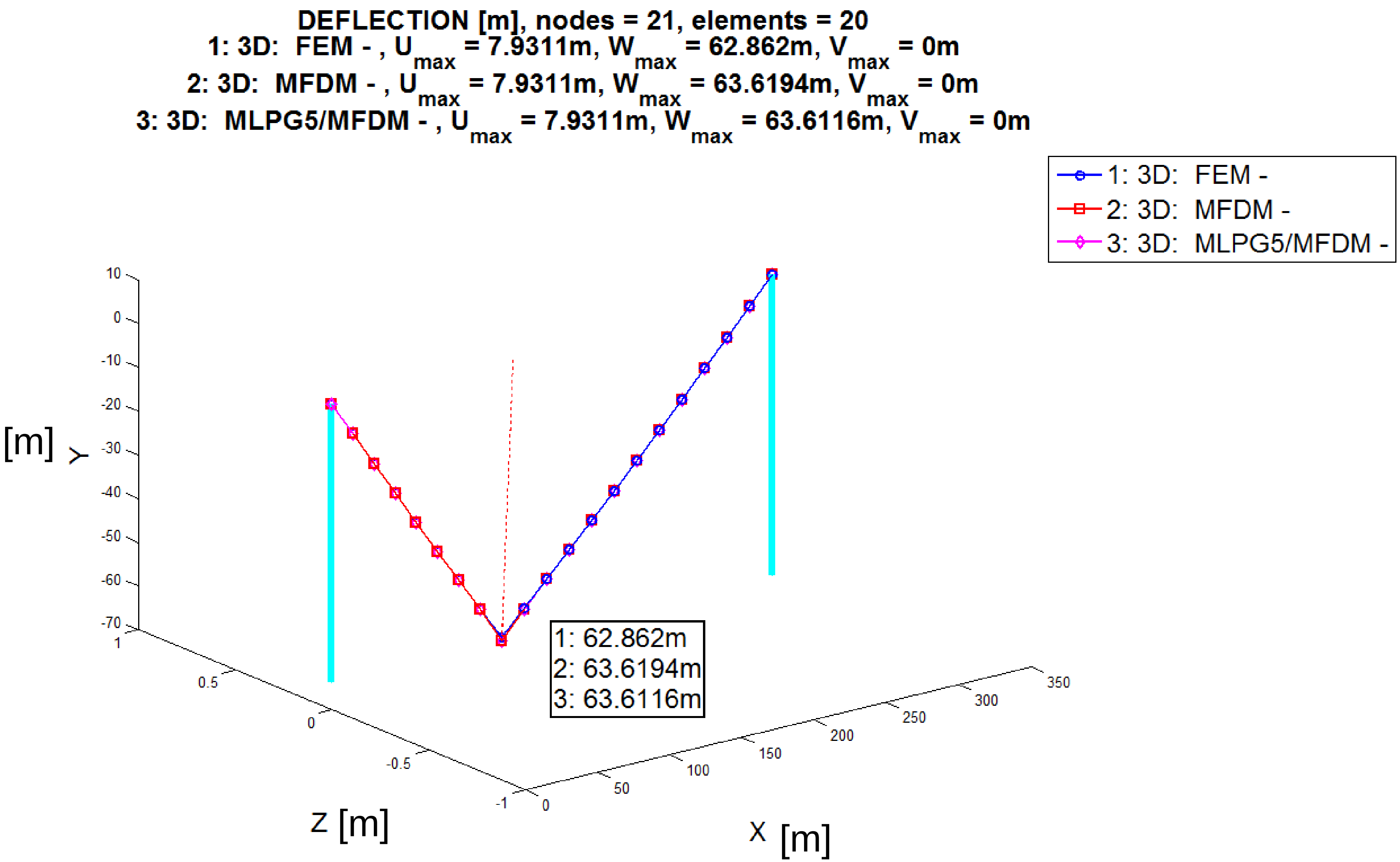

TEST DATA #1 (EP)

Comparison of **methods** 1. FEM , 2. MFDM , 3. MLPG-5/MFDM

313 nodes, computational time, 1: 9s, 2: 20s, 3: 44s

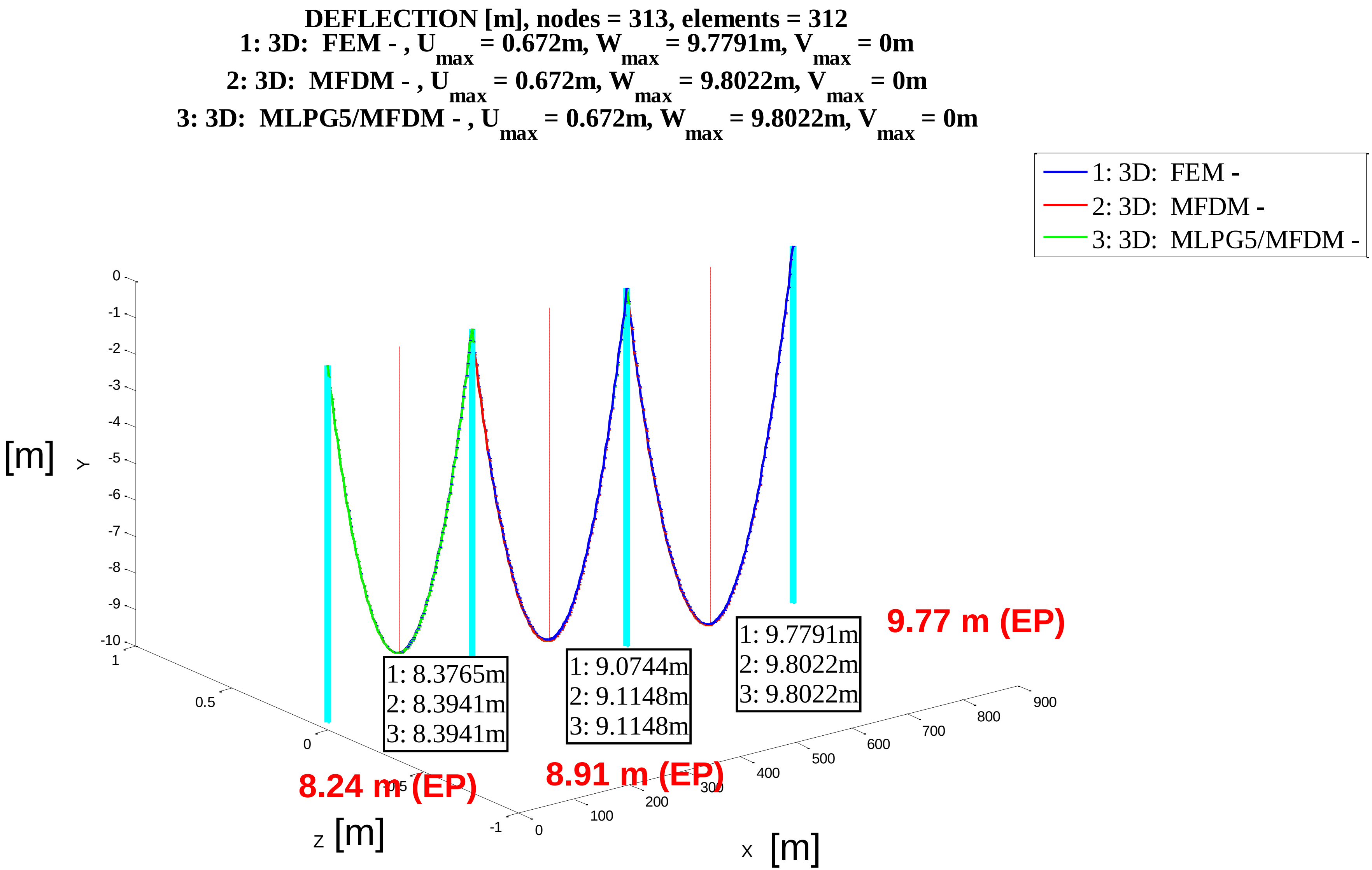

TEST DATA #2 (EP)

FEM , MFDM , MLPG-5/MFDM results **convergence** for regular mesh

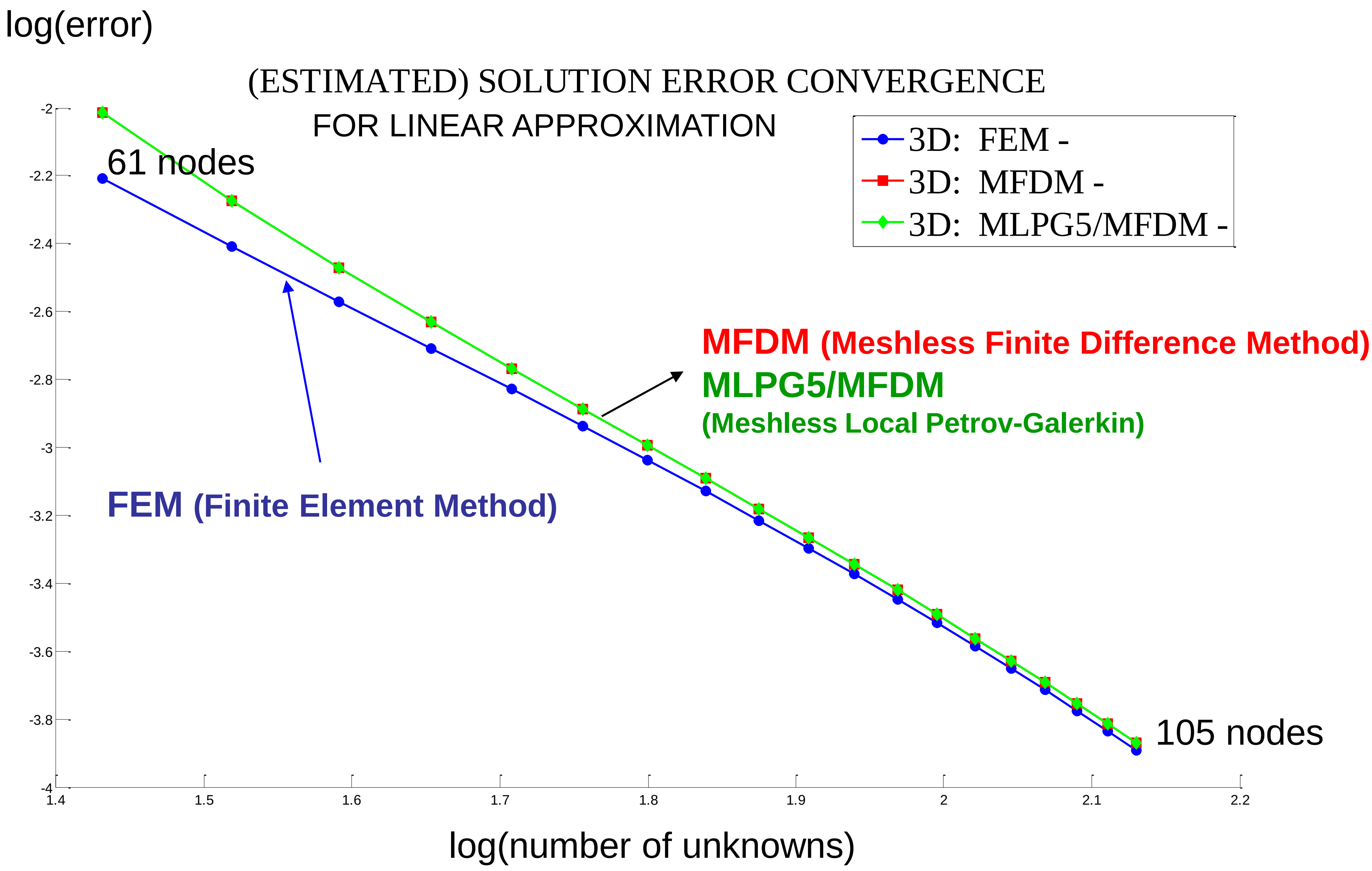

TEST DATA #**1** – distributed loads
MFDM various (1,2,3) **approximation orders**

21 nodes, computational time, 1: 4s, 2: 10s, 3: 20s

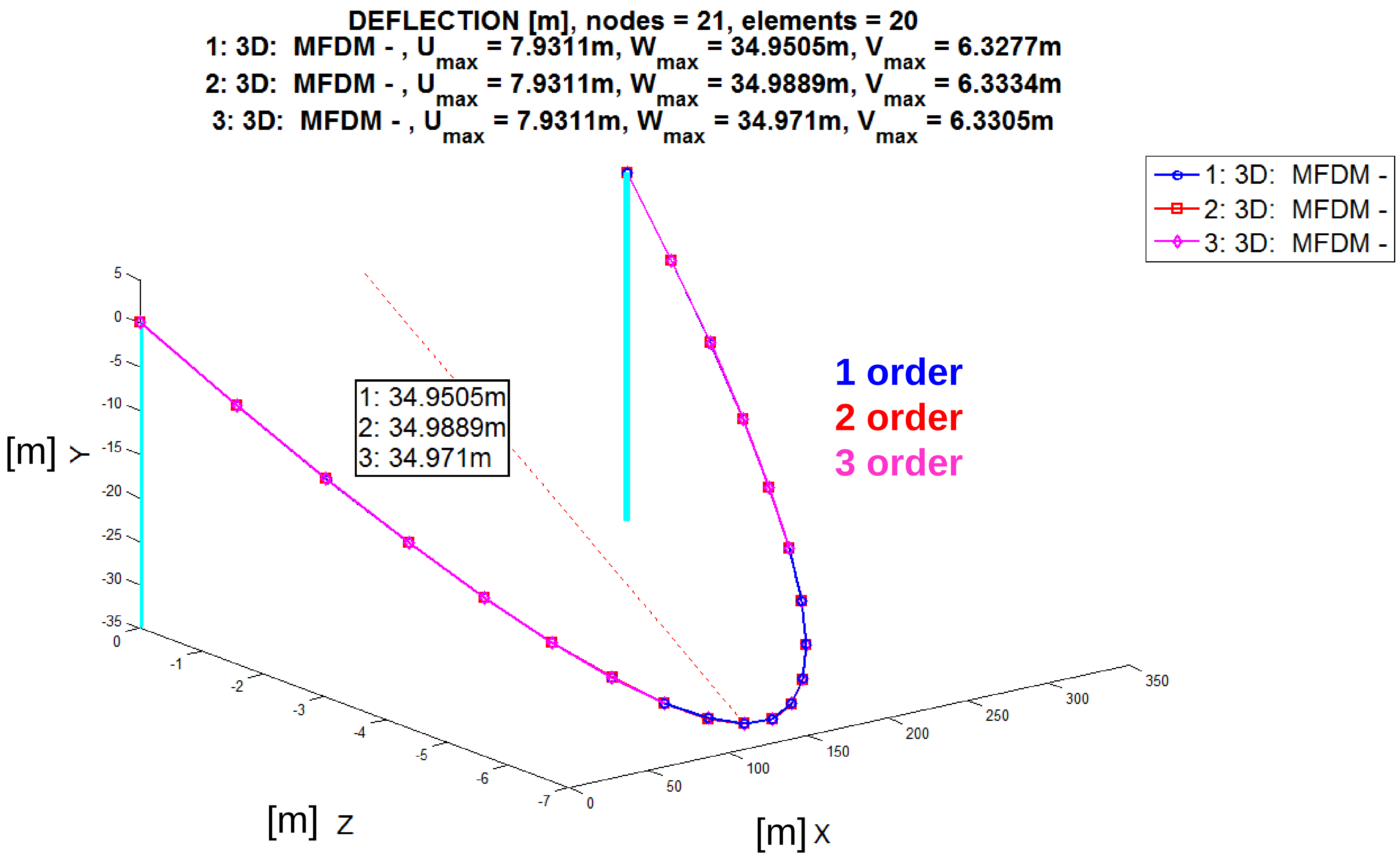

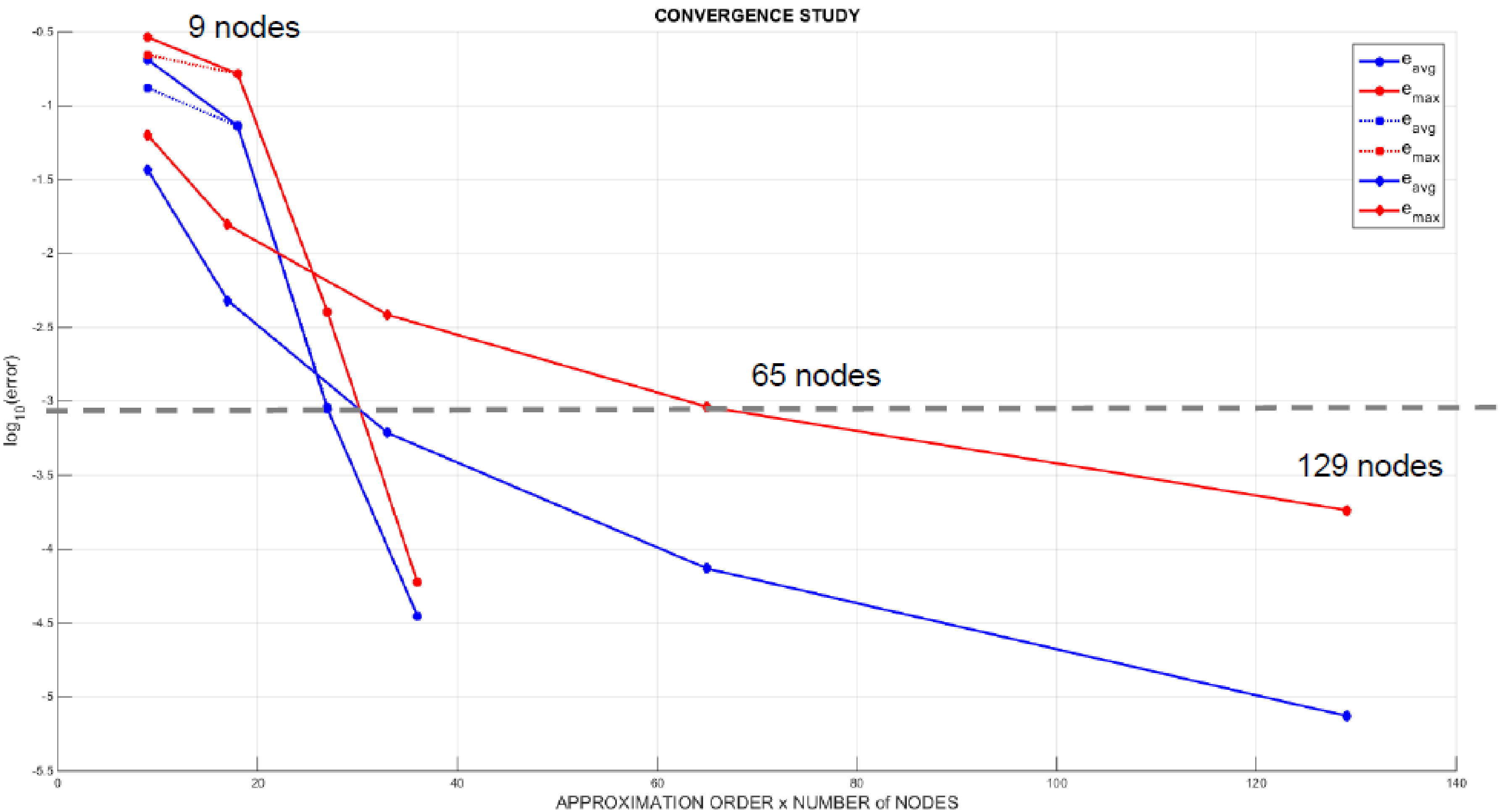

CONVERGENCE STUDY
9 nodes
65 nodes
129 nodes
e_{avg}
e_{max}
e_{avg}
e_{max}
e_{avg}
e_{max}
-0.5
-1
-1.5
-2
-2.5
-3
-3.5
-4
-4.5
-5
-5.5
$log_{10}(error)$
0
20
40
60
80
100
120
140
APPROXIMATION ORDER x NUMBER of NODES

TEST DATA **#2** (EP)

Influence of supporting **structure elasticity** (MFDM)

21 nodes, computational time, 1: 2s, 2: 2s

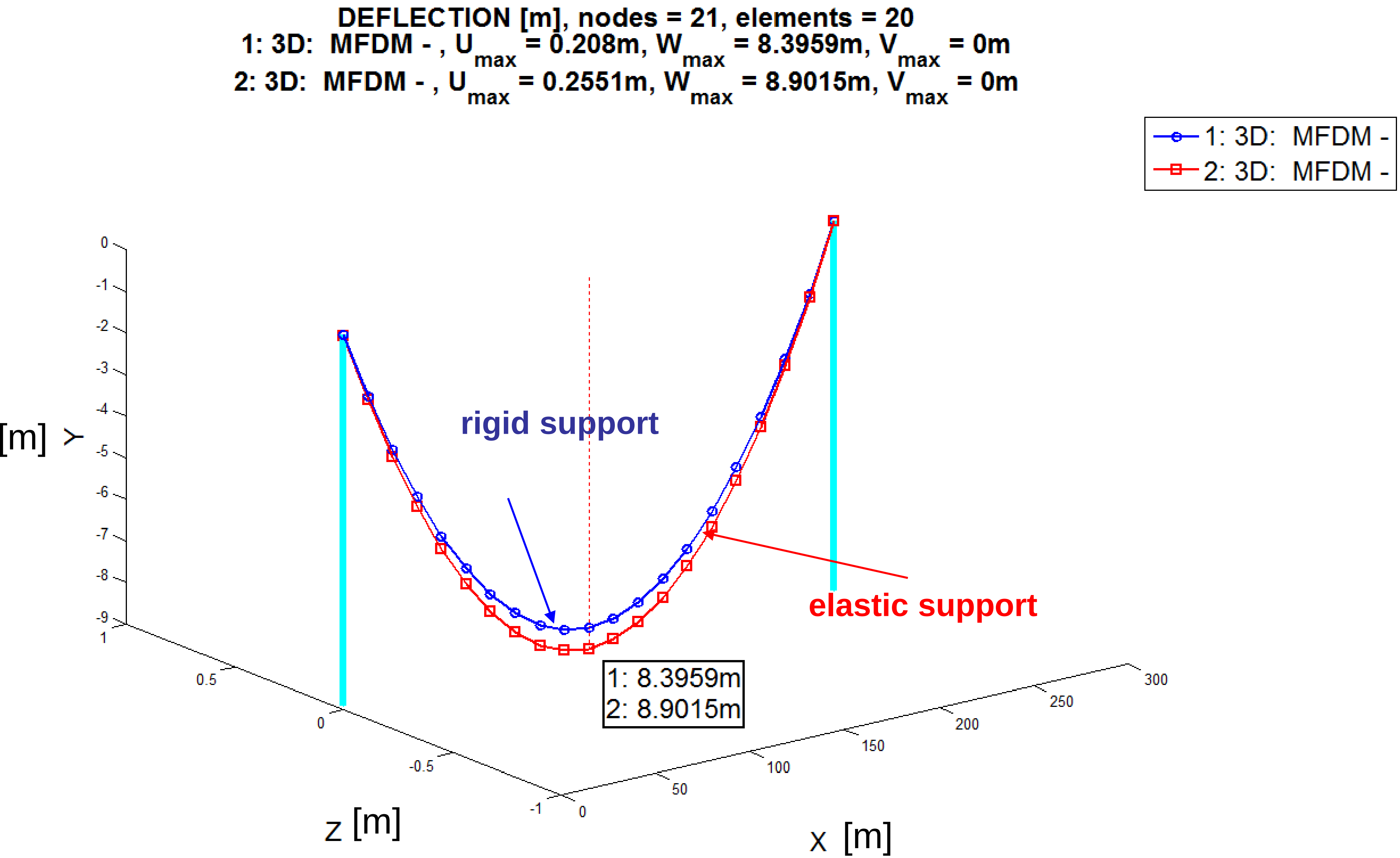

TEST DATA **#2** (EP)

Influence of chains of **insulators** (MFDM)

21 nodes, computational time, 1: 2s, 2: 2s, 3: 2s

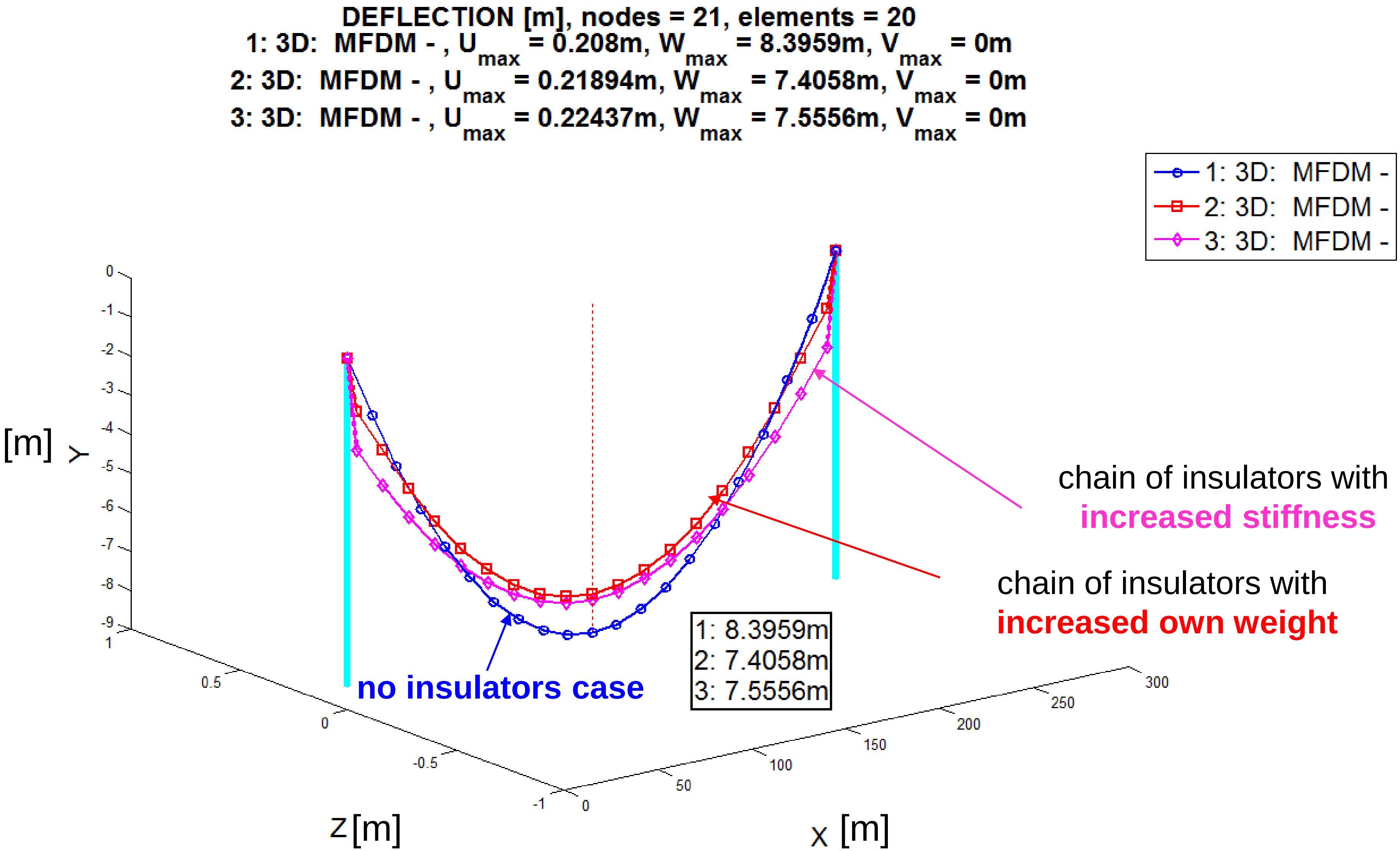

5. HIBRID THEORETICAL – EXPERIMENTAL ANALYSIS OF OVERHEAD POWER TRANSMISSION LINES

Constrained nonlinear optimization problem type B

5.1 Types of on-line **measured data**, and ways of their use

data types

= **weather conditions**, electric **current** induced data $\Rightarrow$ loadings and conductors

= **angles** of conductor **inclination** and **rotation**

chosen **ways** of **use** of measured angles

= **comparison** of **measured** and **calculated data** itself

= cable deflections analysis including measured data

- Approach I: including angle measurements into common **simultaneous hybrid theoretical-experimental-numerical solution** approach

- Approach II: use of measured cable inclination angles to appropriate modification of initial data and solution of cable deflections b.v.problem defined above

5.2 Measurement of cable inclination angles by EC Systems

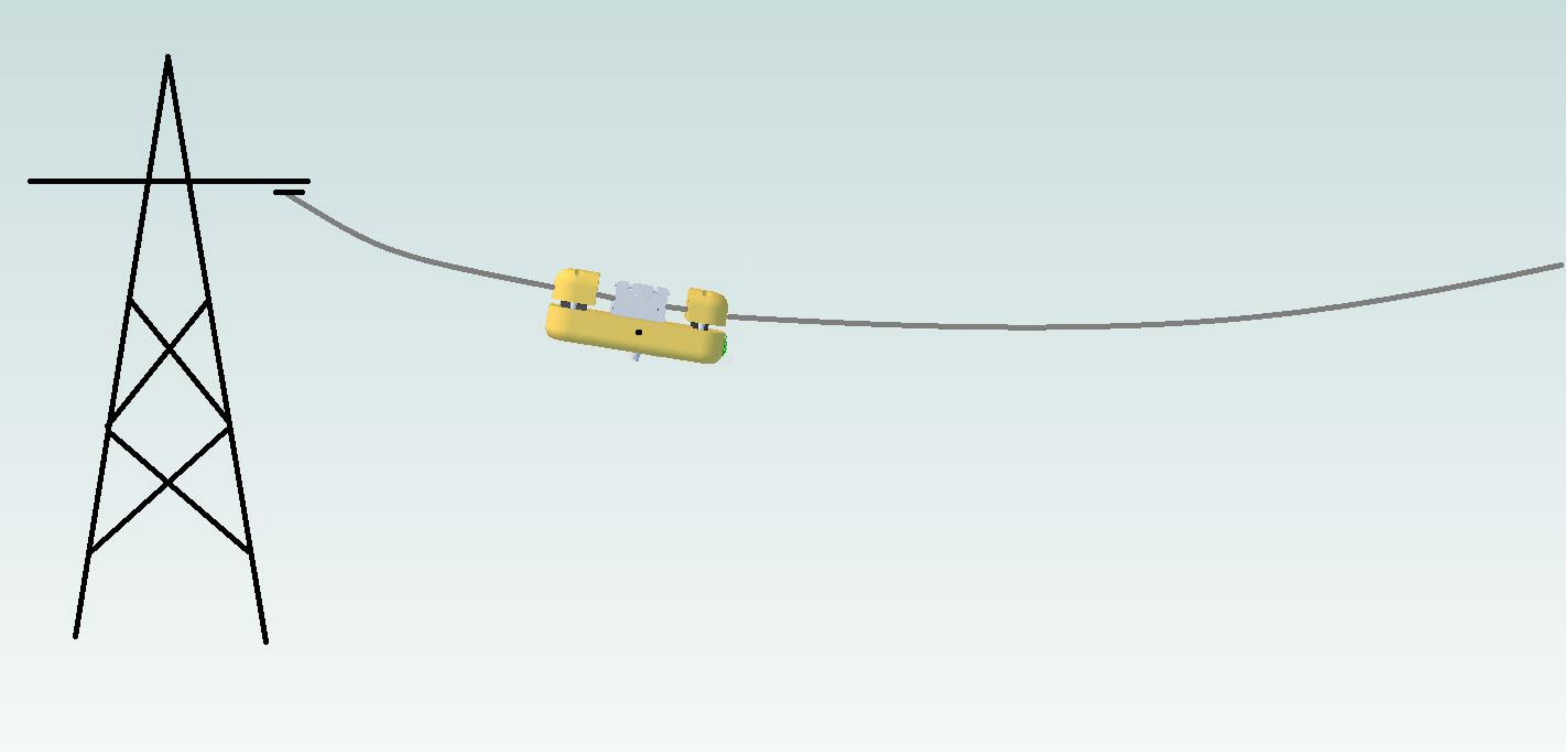

Cable inclination measurement

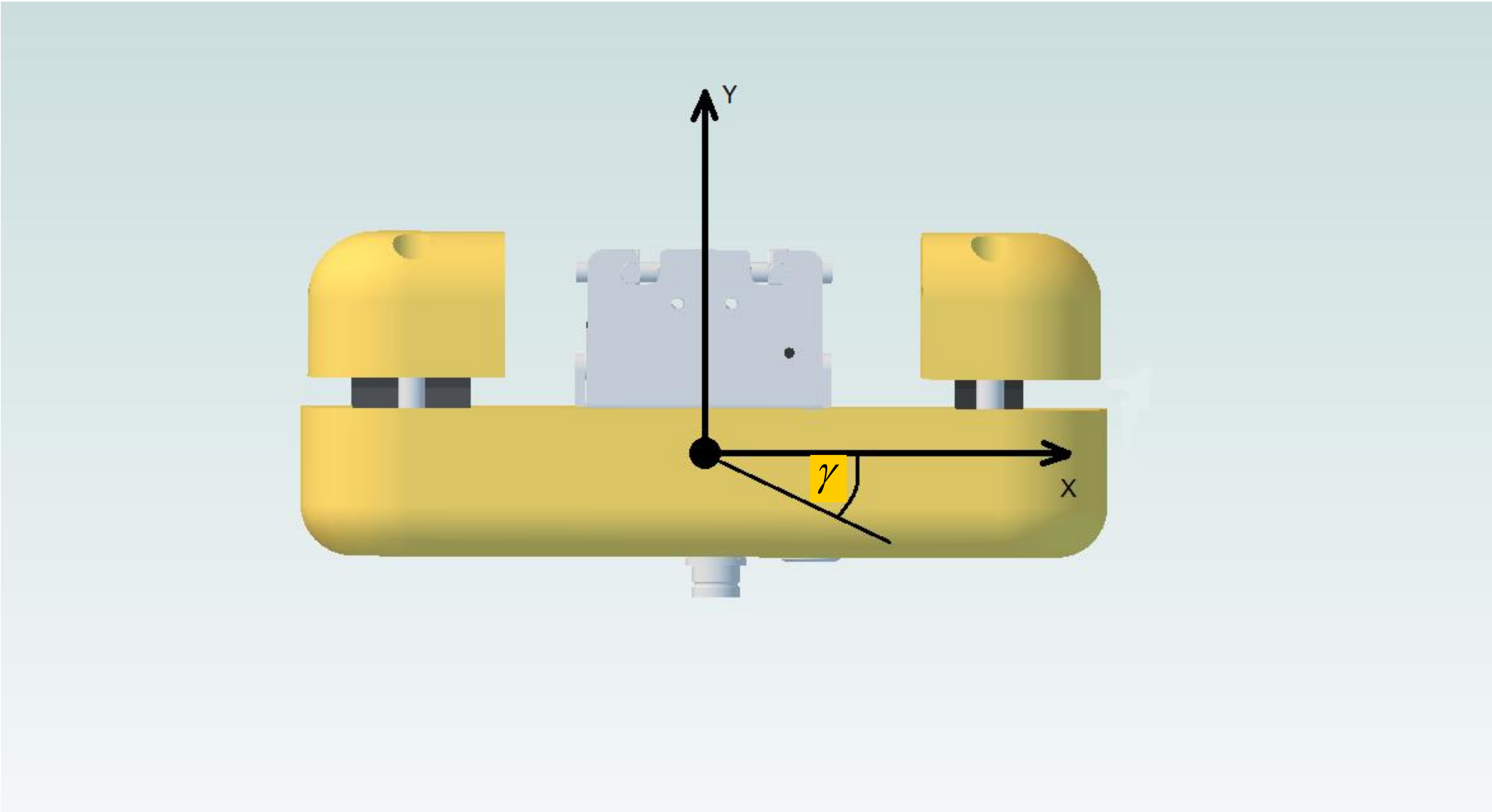

Cable rotation measurement

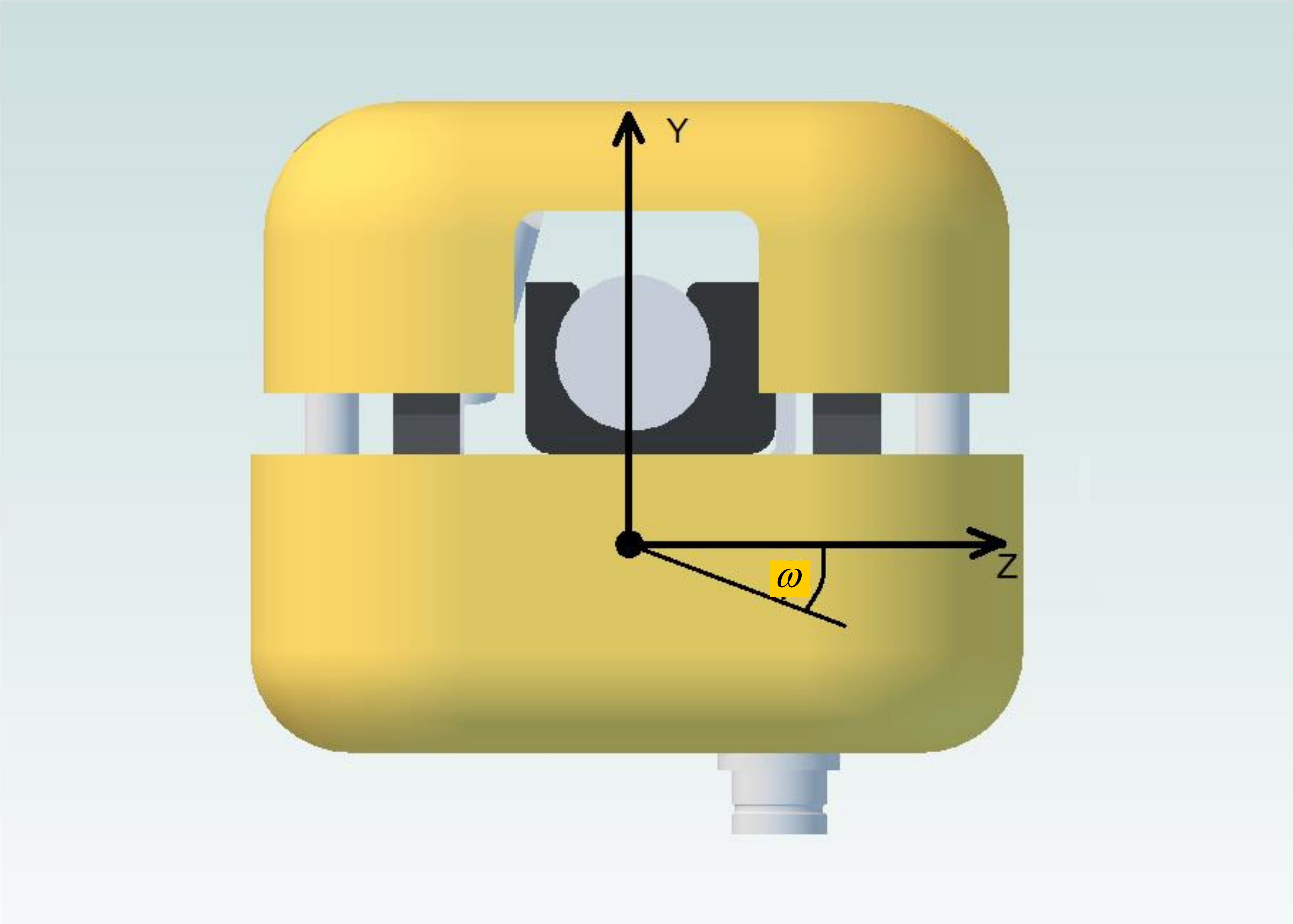

On-line measured angles

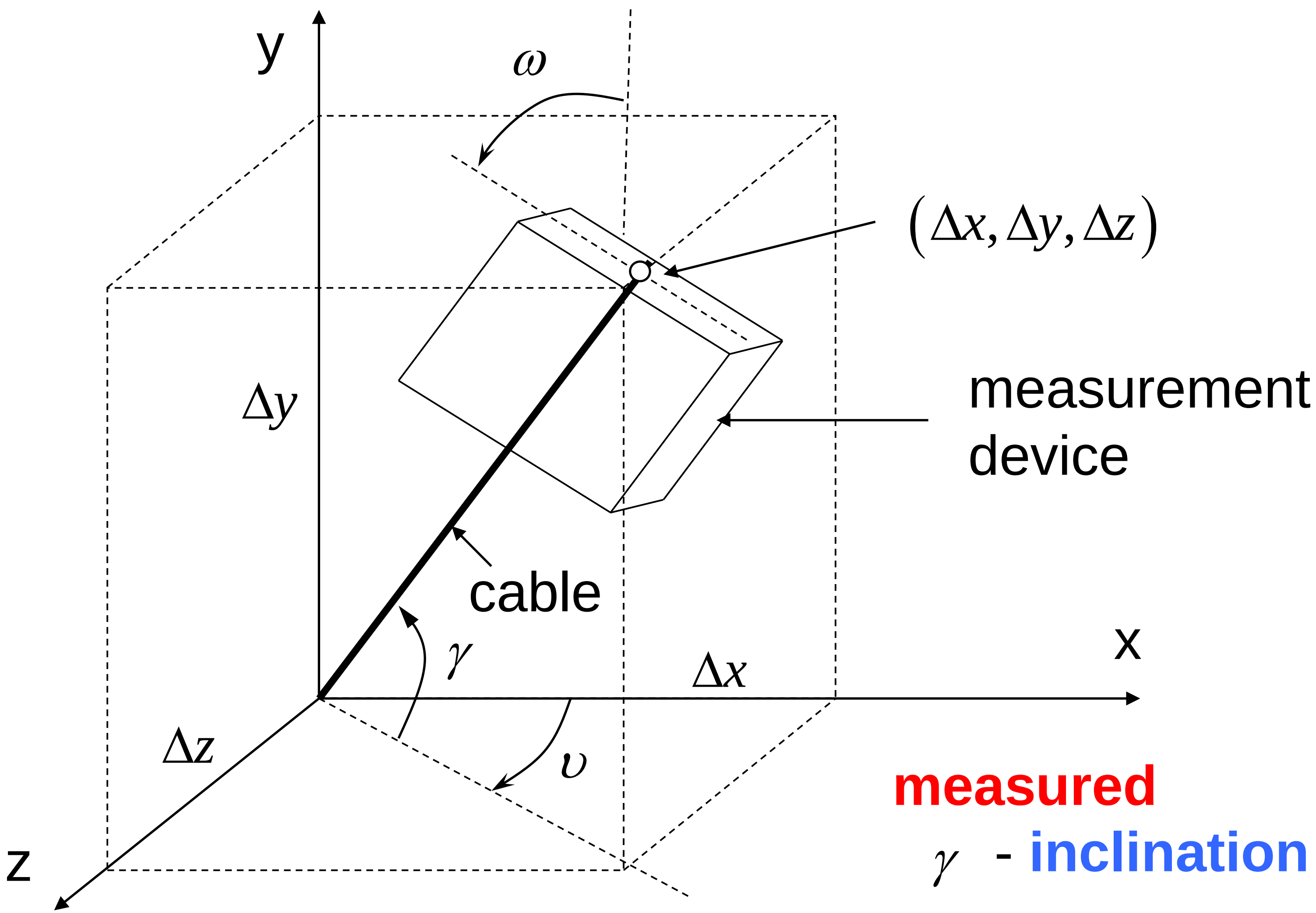

measured

γ - **inclination** angle

$$tg\gamma = \frac{\Delta y}{\sqrt{(\Delta x)^2 + (\Delta z)^2}}$$

ω - **rotation** angle

5.3 HYBRID SOLUTION APPROACH I using the physically based approximation (PBA) for **simultaneous** analysis of **theory** and all **experimental** data

General formulation

find the **stationary point** of the functional

$$\phi(u,\lambda)=\lambda\phi^{T}(u)+(1-\lambda)\phi^{E}(u) \qquad \lambda\in[0,1]$$

satisfying **equality**

and **inequality** **constraints**

$$A(u)=b$$
$$B(u)<e$$

where ϕ^{T} and ϕ^{E} are dimensionless **theoretical** and **experimental** parts of the functional.

Formulation for conductors displacements $\boldsymbol{u}(X)$

Theoretical part - only variational form available

$$\delta\varphi^{T}=\frac{1}{C}\left\{\int_{0}^{L}v'\cdot\mathbf{F}\,dX-\int_{0}^{L}v\cdot\mathbf{p}\,dX+\sum_{k}^{2}v_{k}^{T}\cdot\mathbf{K}_{k}^{(s)}(u_{k}-\hat{u}_{k})\right\}$$

C – parameter for unitless variational form

Experimental part – for measured inclination γ^{E} and rotation ω^{E} angles as well as displacements

$$\phi^{E}=\frac{1}{J+2K}\sum_{k=1}^{K}\left\{\left[\frac{tg\gamma_{k}-tg\gamma_{k}^{E}}{e_{\gamma_{k}}}\right]^{2}+\left[\frac{tg\omega_{k}-tg\omega_{k}^{E}}{e_{\omega_{k}}}\right]^{2}\right\}+\sum_{j=1}^{J}\left(\frac{\left\|P_{j}-P_{j}^{E}\right\|}{e_{P_{j}}}\right)^{2},$$

$$\left\|P_{j}-P_{j}^{E}\right\|^{2}=\left(x_{j}-x_{j}^{E}\right)^{2}+\left(y_{j}-y_{j}^{E}\right)^{2}+\left(w_{j}-w_{j}^{E}\right)^{2}$$

Two steps **solution procedure**

(i) solve

$$\delta\varphi = \lambda\delta\varphi^T + (1-\lambda)\delta\varphi^E = 0 \quad \rightarrow \quad \boldsymbol{u}(X,\lambda)$$

(ii) find $\lambda_{\max}$ for $\boldsymbol{u}(X,\lambda)$, $\lambda \in [0,\ 1]$

satisfying **inequality constraints**

local error

$$\left|\frac{tg\gamma_k - tg\gamma_k^E}{e_{\gamma_k}}\right| \le 1 \quad , \quad \left|\frac{tg\omega_k - tg\omega_k^E}{e_{\omega_k}}\right| \le 1 \quad , \quad \frac{\left\|P_j - P_j^E\right\|^2}{e_{P_j}^2} \le 1 \ , \quad j = 1,2,\ldots,J, \quad k = 1,2,\ldots,K$$

global error

$$\sqrt{\Phi^E} < \frac{1}{m}, \quad m \ge 1,\ m \approx 2 \div 5$$

where

$$tg\gamma_i^T = \frac{1}{\Delta}\int_\Delta tg\gamma dX = \frac{1}{\Delta}\int_\Delta \frac{y'}{\sqrt{(x')^2 + (z')^2}} dX \approx \frac{\Delta y}{\sqrt{(\Delta x)^2 + (\Delta z)^2}}$$

$$tg\omega_i^T = \frac{1}{\Delta}\int_\Delta tg\omega dX = \qquad \approx h(\Delta x, \Delta y, \Delta z)$$

may be expressed in terms of unknown $\boldsymbol{u}$ quantities

e_{γ_k} , e_{ω_k} , e_{P_j} admissible **measurement tolerances**

OPTIMIZATION PROCEDURE FOR VARIABLE CABLE LENGTH L AND TEMPERATURE T

1. solve above FBA problem assuming fixed values $T = T^E$ and $L = L^E$

2. fix $T = T^E$ vary L , find $L = L_{opt}$

minimising cable curvature and satisfying the constraint

$$\min_L \kappa^2 \quad , \quad \kappa^2 \approx \frac{1}{L}\int_0^L \left(\frac{d^2 w}{dX^2}\right)^2 dX \qquad \Delta L = \left|L - L^E\right| \le e_L = \Delta L_{\max}$$

3. fix $L = L_{opt}$ vary T , find $T = T_{opt}$

minimising the same cable curvature κ^2 while satisfying constraints $\Delta T = \left|T - T^E\right| \le e_T = \Delta T_{\max}$

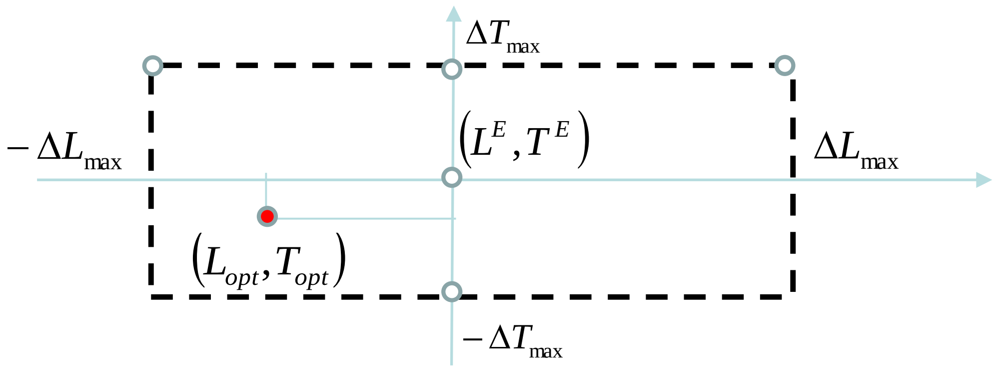

5.4 Accounting for measurement data - approach II

Whenever $|\omega^E - \frac{1}{\Delta}\int_\Delta \omega(T^E, \hat{L}, \hat{q}, \hat{p})\,\mathrm{d}X| > e_\omega$

$$\left[T^E, \hat{L}, \hat{q}, \hat{p}\right] = \hat{\boldsymbol{Z}} \;\rightarrow\; \tilde{\boldsymbol{Z}} = \left[\tilde{T}, \tilde{L}, \tilde{q}, \tilde{p}\right]$$

$$J(\boldsymbol{Z}) = \alpha_\omega \left[\int_\Delta \omega(\boldsymbol{Z})\,\mathrm{d}X - \omega^E \Delta\right]^2 + \alpha_T (T - T^E)^2$$

α_ω, α_T − **appropriate weights**

$J(\tilde{\boldsymbol{Z}}) = \min_{\boldsymbol{Z}} J(\boldsymbol{Z})$ **subject to** $|\tilde{Z}_i - \hat{Z}_i| \leqslant e_z$

$$\boldsymbol{u} = \boldsymbol{u}(\tilde{T}, \tilde{L}, \tilde{q}, \tilde{p})$$

Other measured quantities, like angle γ or wind q may be also considered in $J(Z)$.

TEST DATA **#2** (EP) – **Approach I**

Influence of measurement data (MFDM)

21 nodes, computational time, 1: 1s, 2: 1s, 3: 18s

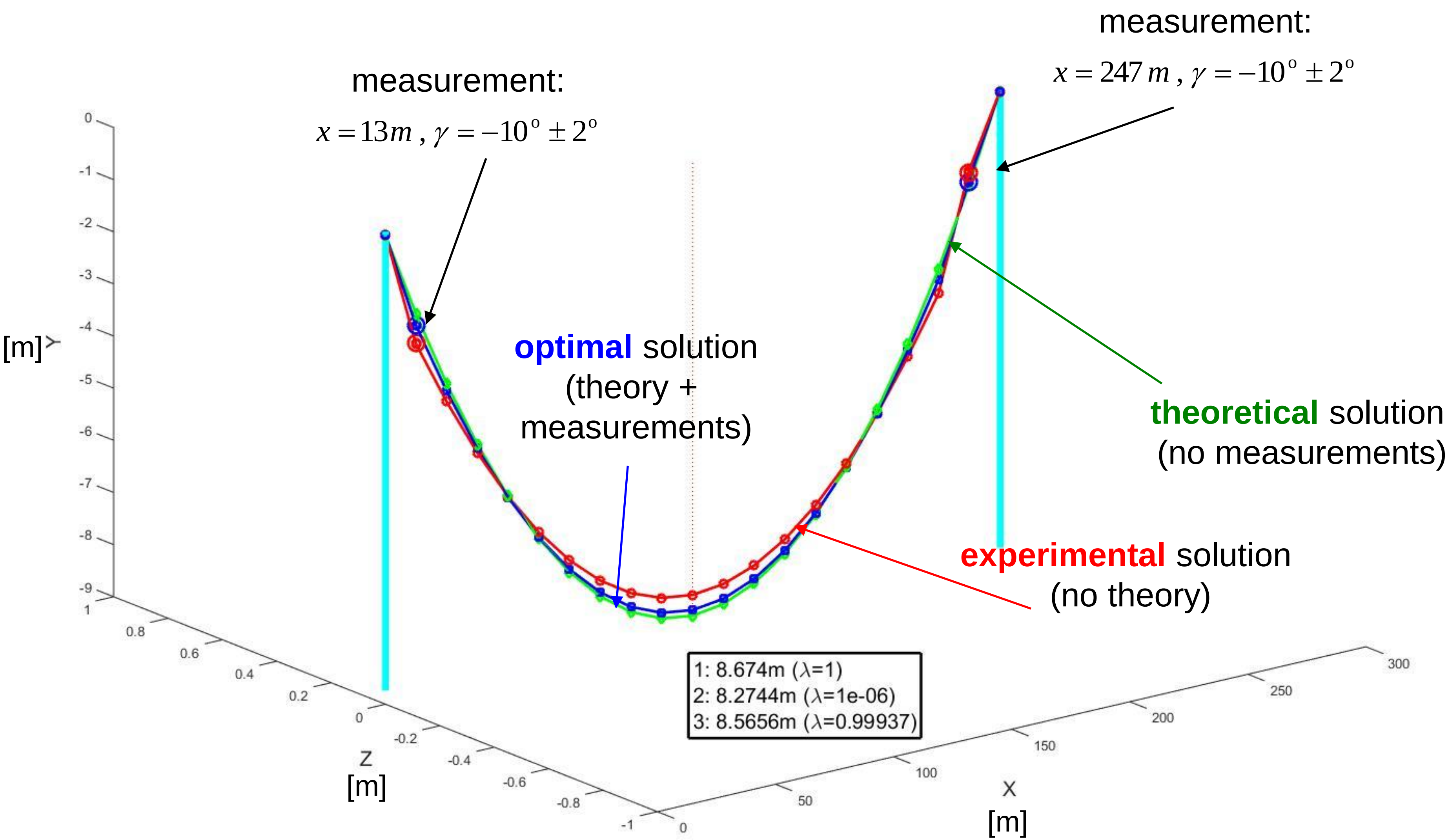

TEST DATA #2 (EP) – Approach I

Influence of measurement data (MFDM)

21 nodes, computational time, 1: 1s, 2: 17s, 3: 17s

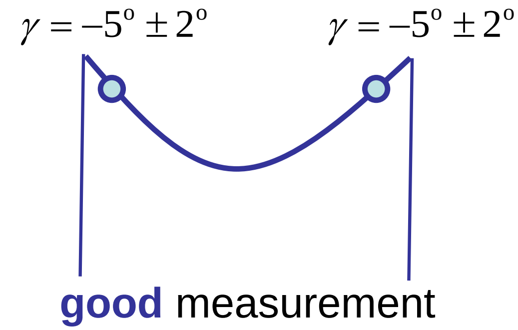

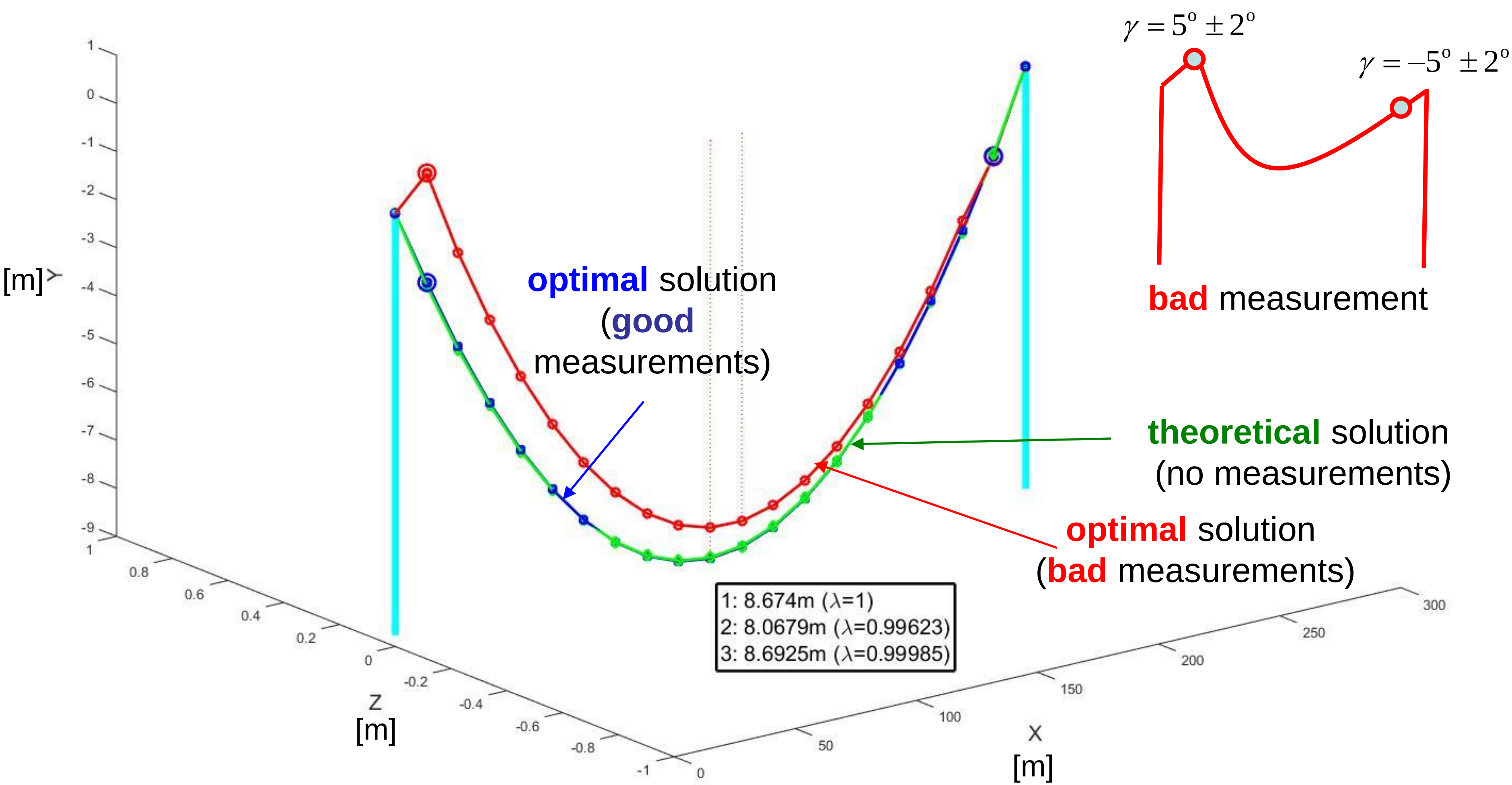

TEST DATA **#2** (EP) – **Approach I** against **Approach II**

Influence of measurement data (MFDM – approach I, FEM – approach II)

21 nodes, computational time, 1: 1s, 2: 18s, 3: 1s

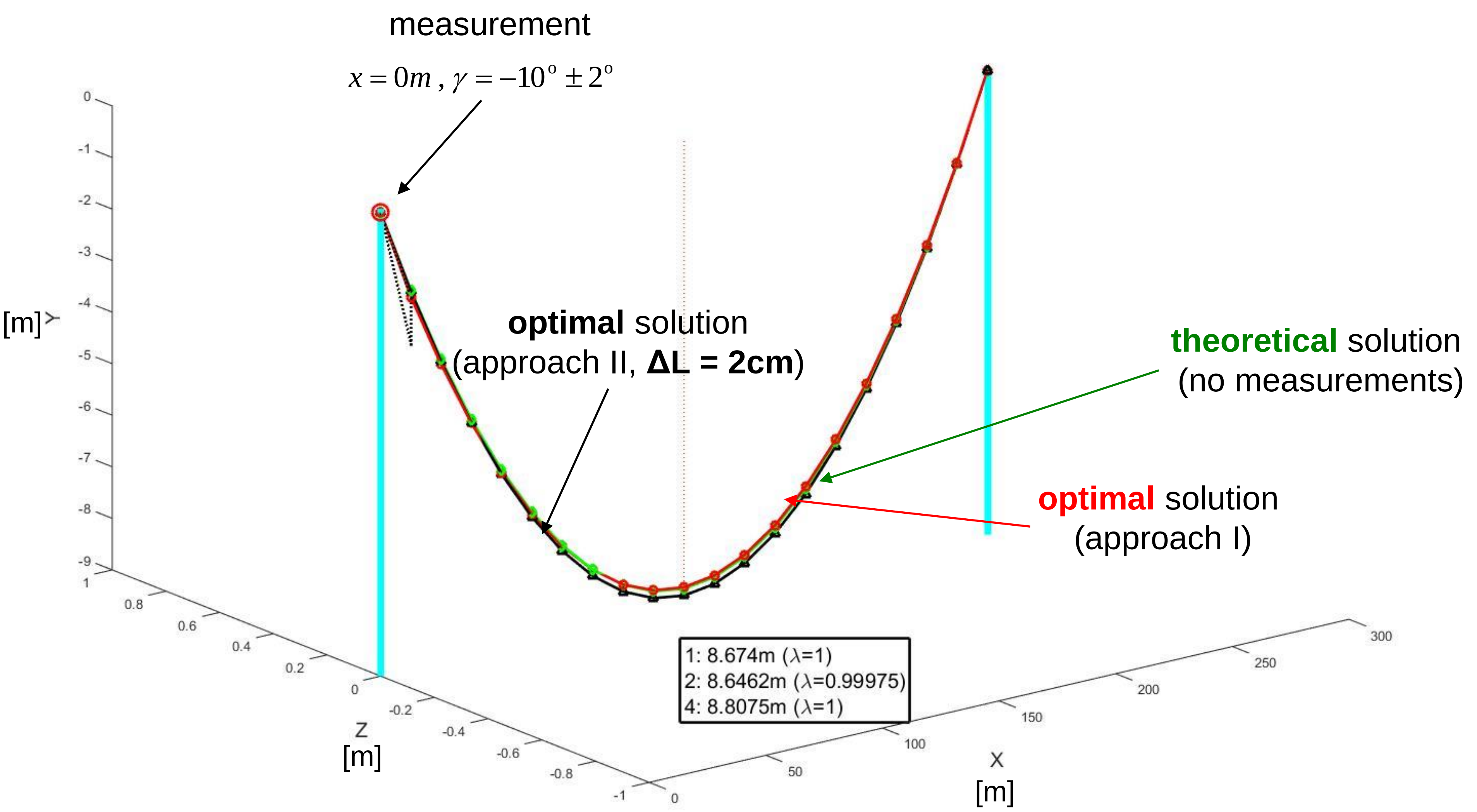

TEST DATA #2 (EP) – Approach I against Approach II

Influence of measurement data (MFDM – approach I, FEM – approach II)

21 nodes, computational time, 1: 1s, 2: 18s, 3: 1s

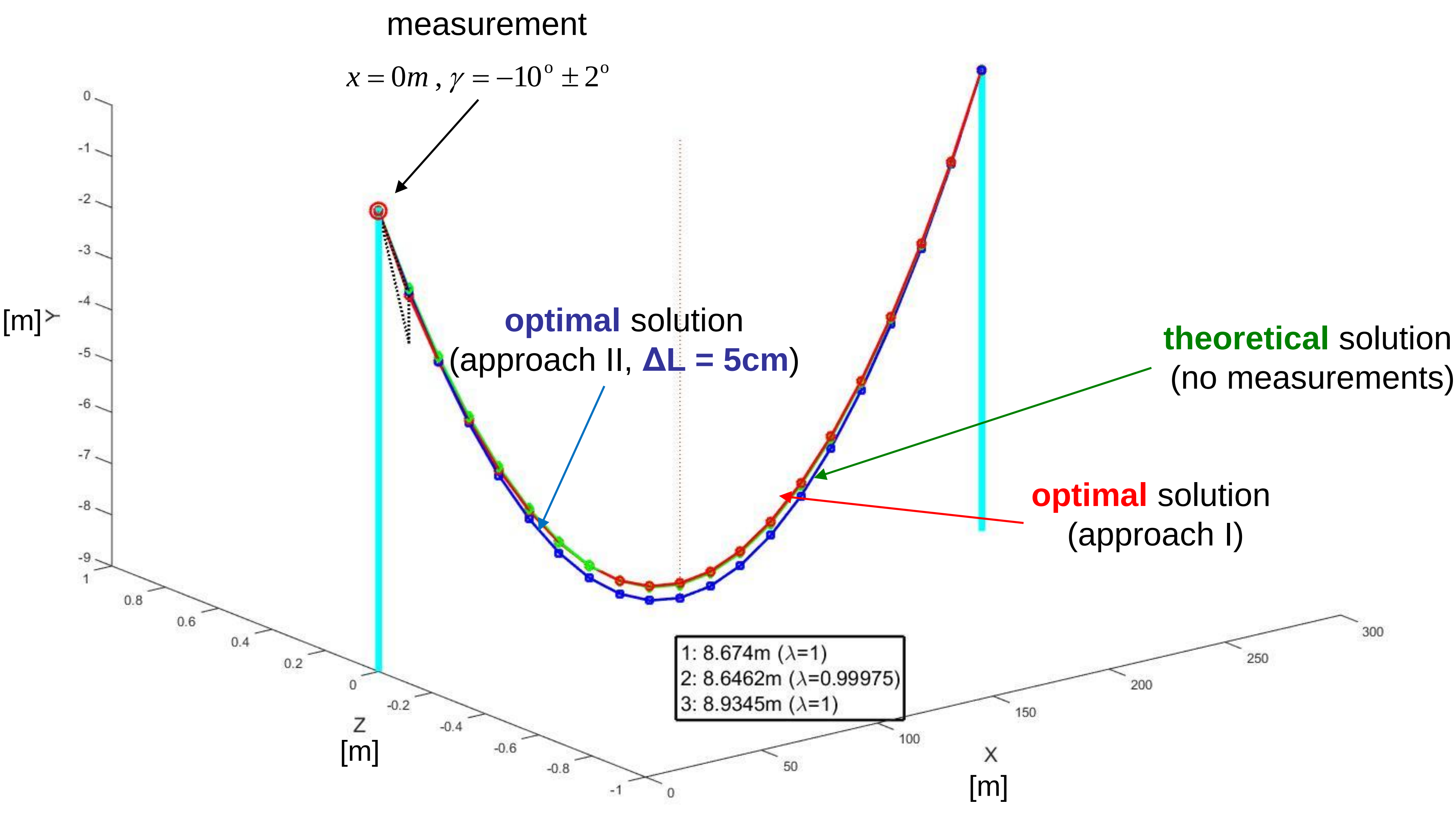

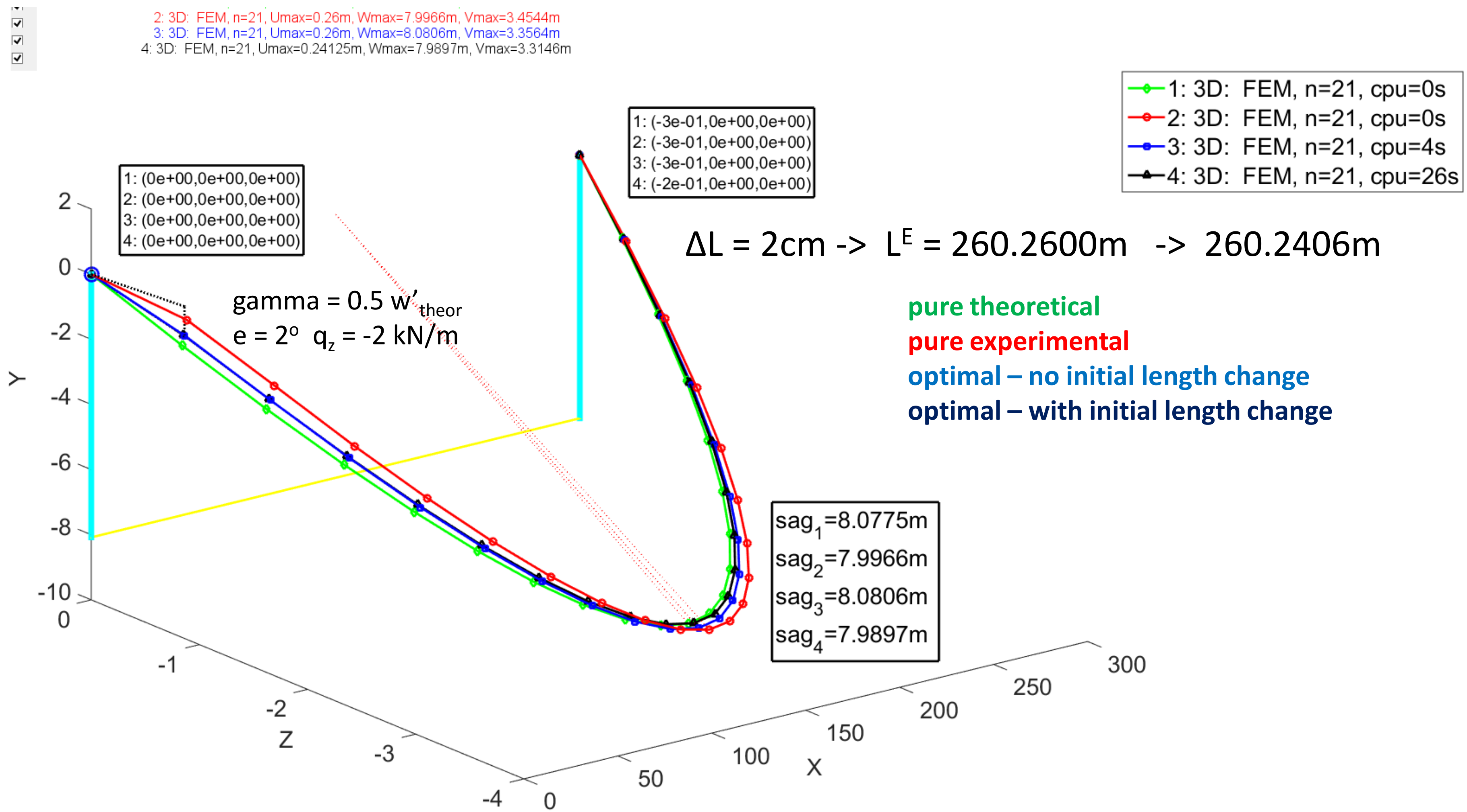

2: 3D: FEM, n=21, Umax=0.26m, Wmax=7.9966m, Vmax=3.4544m
3: 3D: FEM, n=21, Umax=0.26m, Wmax=8.0806m, Vmax=3.3564m
4: 3D: FEM, n=21, Umax=0.24125m, Wmax=7.9897m, Vmax=3.3146m
1: 3D: FEM, n=21, cpu=0s
2: 3D: FEM, n=21, cpu=0s
3: 3D: FEM, n=21, cpu=4s
4: 3D: FEM, n=21, cpu=26s
1: (0e+00,0e+00,0e+00)
2: (0e+00,0e+00,0e+00)
3: (0e+00,0e+00,0e+00)
4: (0e+00,0e+00,0e+00)
1: (-3e-01,0e+00,0e+00)
2: (-3e-01,0e+00,0e+00)
3: (-3e-01,0e+00,0e+00)
4: (-2e-01,0e+00,0e+00)
ΔL = 2cm -> L^E = 260.2600m -> 260.2406m
gamma = 0.5 w'_{theor}
e = 2° q_z = -2 kN/m
pure theoretical
pure experimental
optimal – no initial length change
optimal – with initial length change
sag_1=8.0775m
sag_2=7.9966m
sag_3=8.0806m
sag_4=7.9897m
Y
Z
X

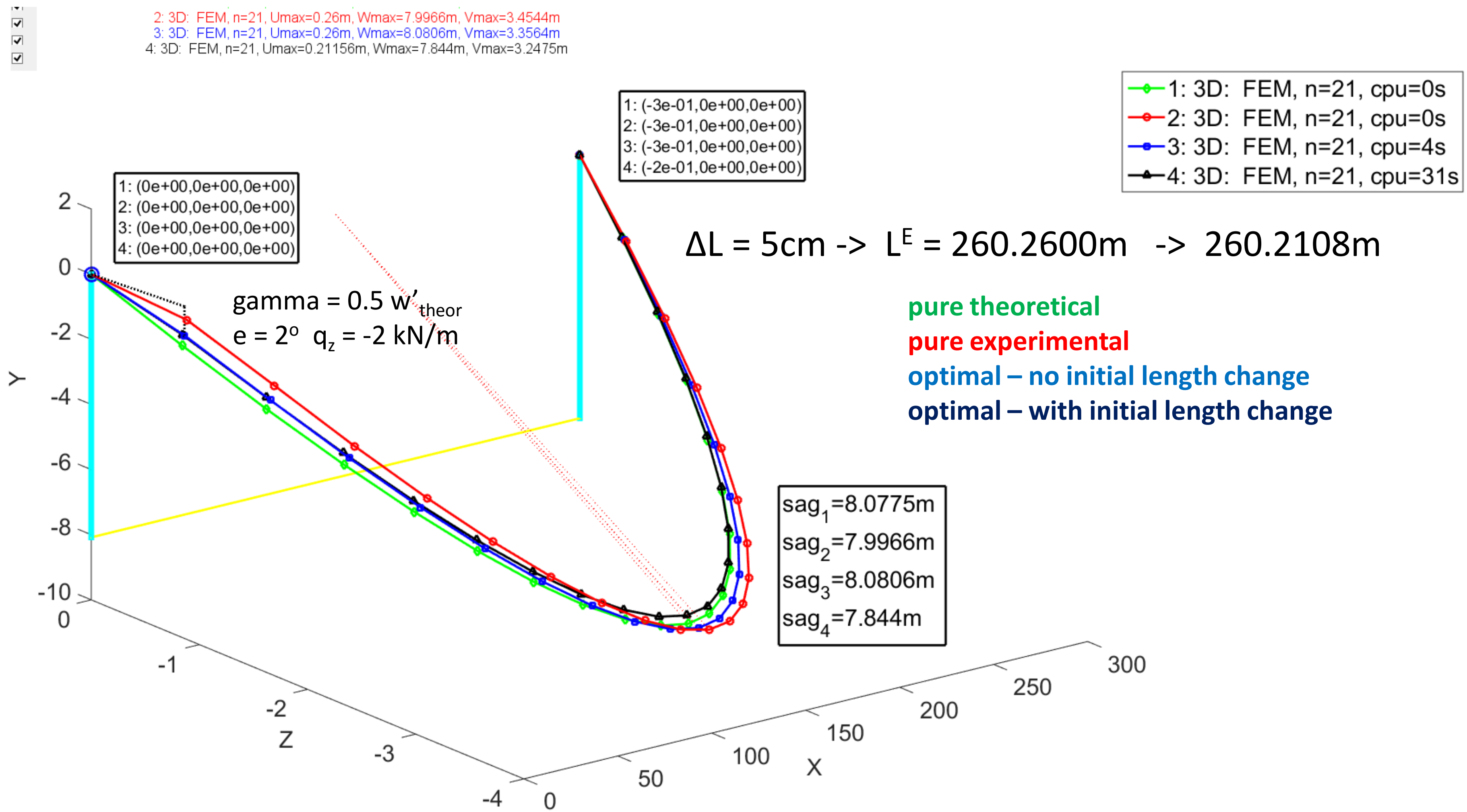
2: 3D: FEM, n=21, Umax=0.26m, Wmax=7.9966m, Vmax=3.4544m
3: 3D: FEM, n=21, Umax=0.26m, Wmax=8.0806m, Vmax=3.3564m
4: 3D: FEM, n=21, Umax=0.21156m, Wmax=7.844m, Vmax=3.2475m
1: 3D: FEM, n=21, cpu=0s
2: 3D: FEM, n=21, cpu=0s
3: 3D: FEM, n=21, cpu=4s
4: 3D: FEM, n=21, cpu=31s
1: (-3e-01,0e+00,0e+00)
2: (-3e-01,0e+00,0e+00)
3: (-3e-01,0e+00,0e+00)
4: (-2e-01,0e+00,0e+00)
1: (0e+00,0e+00,0e+00)
2: (0e+00,0e+00,0e+00)
3: (0e+00,0e+00,0e+00)
4: (0e+00,0e+00,0e+00)
ΔL = 5cm -> L^E = 260.2600m -> 260.2108m
gamma = 0.5 w'theor
e = 2° qz = -2 kN/m
pure theoretical
pure experimental
optimal – no initial length change
optimal – with initial length change
sag1=8.0775m
sag2=7.9966m
sag3=8.0806m
sag4=7.844m
Y
Z
X

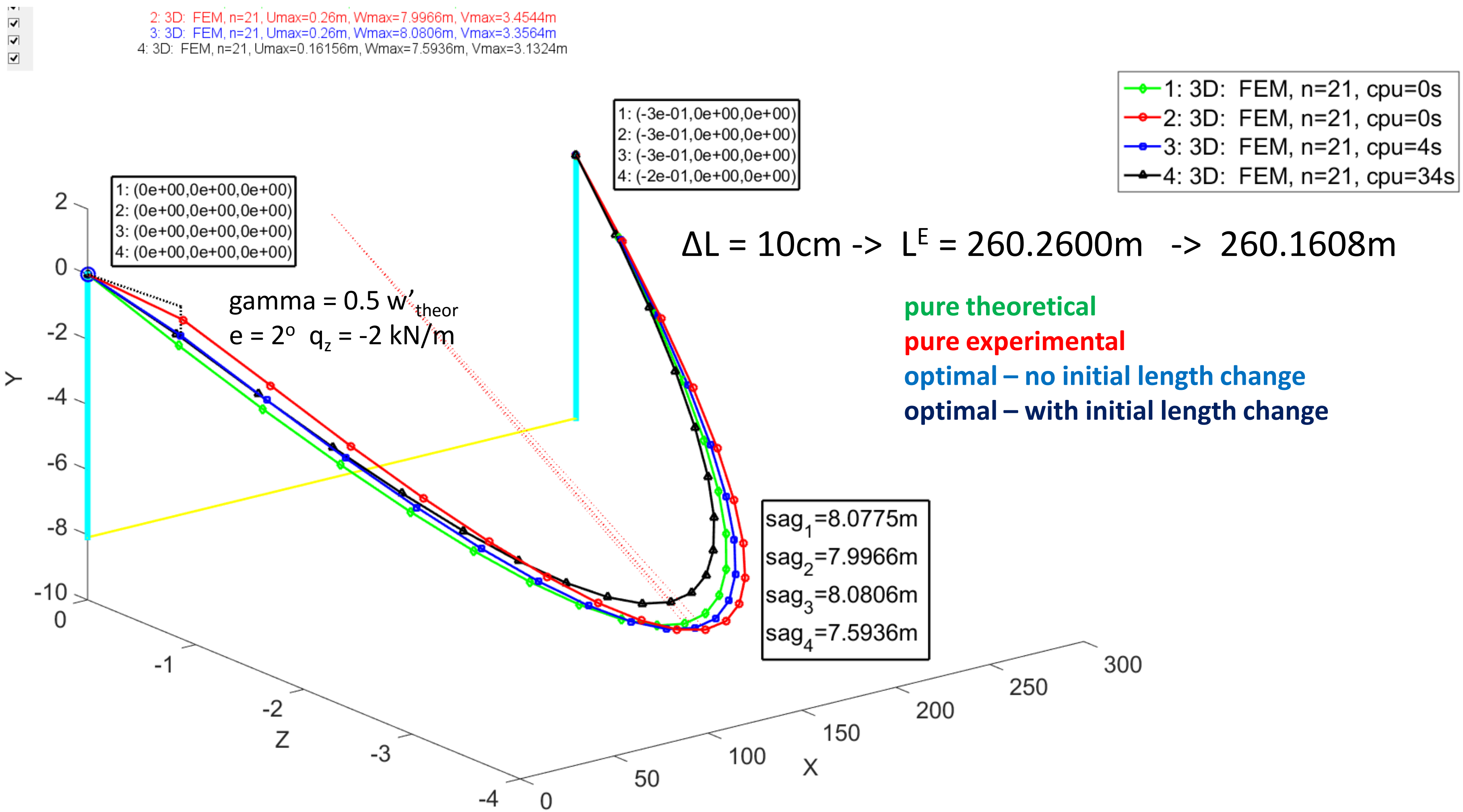

2: 3D: FEM, n=21, Umax=0.26m, Wmax=7.9966m, Vmax=3.4544m
3: 3D: FEM, n=21, Umax=0.26m, Wmax=8.0806m, Vmax=3.3564m
4: 3D: FEM, n=21, Umax=0.16156m, Wmax=7.5936m, Vmax=3.1324m
1: 3D: FEM, n=21, cpu=0s
2: 3D: FEM, n=21, cpu=0s
3: 3D: FEM, n=21, cpu=4s
4: 3D: FEM, n=21, cpu=34s
1: (-3e-01,0e+00,0e+00)
2: (-3e-01,0e+00,0e+00)
3: (-3e-01,0e+00,0e+00)
4: (-2e-01,0e+00,0e+00)
1: (0e+00,0e+00,0e+00)
2: (0e+00,0e+00,0e+00)
3: (0e+00,0e+00,0e+00)
4: (0e+00,0e+00,0e+00)
ΔL = 10cm -> L^E = 260.2600m -> 260.1608m
gamma = 0.5 w'_{theor}
e = 2° q_z = -2 kN/m
pure theoretical
pure experimental
optimal – no initial length change
optimal – with initial length change
sag_1=8.0775m
sag_2=7.9966m
sag_3=8.0806m
sag_4=7.5936m
Y
Z
X

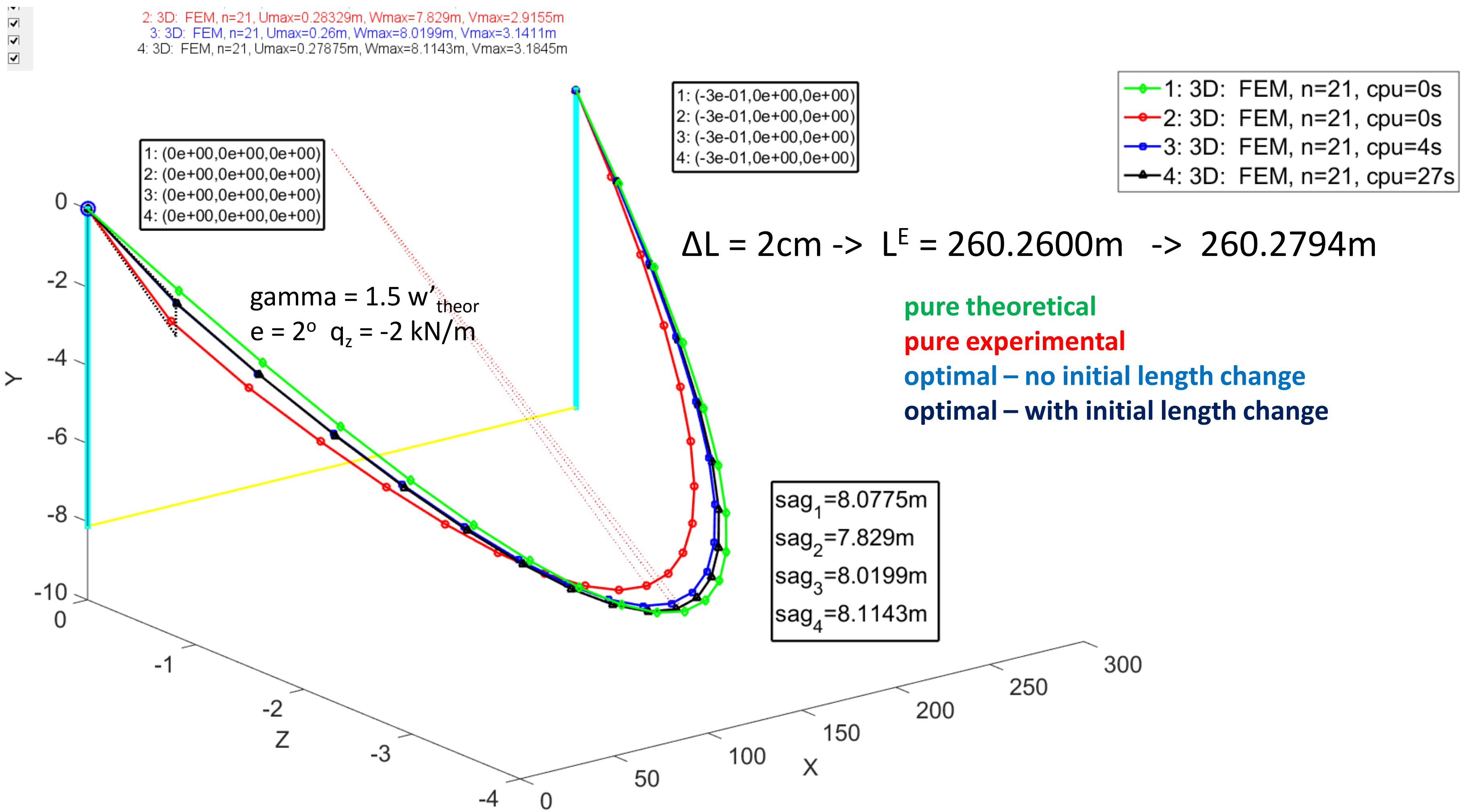
2: 3D: FEM, n=21, Umax=0.28329m, Wmax=7.829m, Vmax=2.9155m
3: 3D: FEM, n=21, Umax=0.26m, Wmax=8.0199m, Vmax=3.1411m
4: 3D: FEM, n=21, Umax=0.27875m, Wmax=8.1143m, Vmax=3.1845m
1: (0e+00,0e+00,0e+00)
2: (0e+00,0e+00,0e+00)
3: (0e+00,0e+00,0e+00)
4: (0e+00,0e+00,0e+00)
1: (-3e-01,0e+00,0e+00)
2: (-3e-01,0e+00,0e+00)
3: (-3e-01,0e+00,0e+00)
4: (-3e-01,0e+00,0e+00)
1: 3D: FEM, n=21, cpu=0s
2: 3D: FEM, n=21, cpu=0s
3: 3D: FEM, n=21, cpu=4s
4: 3D: FEM, n=21, cpu=27s
ΔL = 2cm -> L^E = 260.2600m -> 260.2794m
gamma = 1.5 w'_theor
e = 2° q_z = -2 kN/m
pure theoretical
pure experimental
optimal – no initial length change
optimal – with initial length change
sag_1=8.0775m
sag_2=7.829m
sag_3=8.0199m
sag_4=8.1143m
Y
Z
X

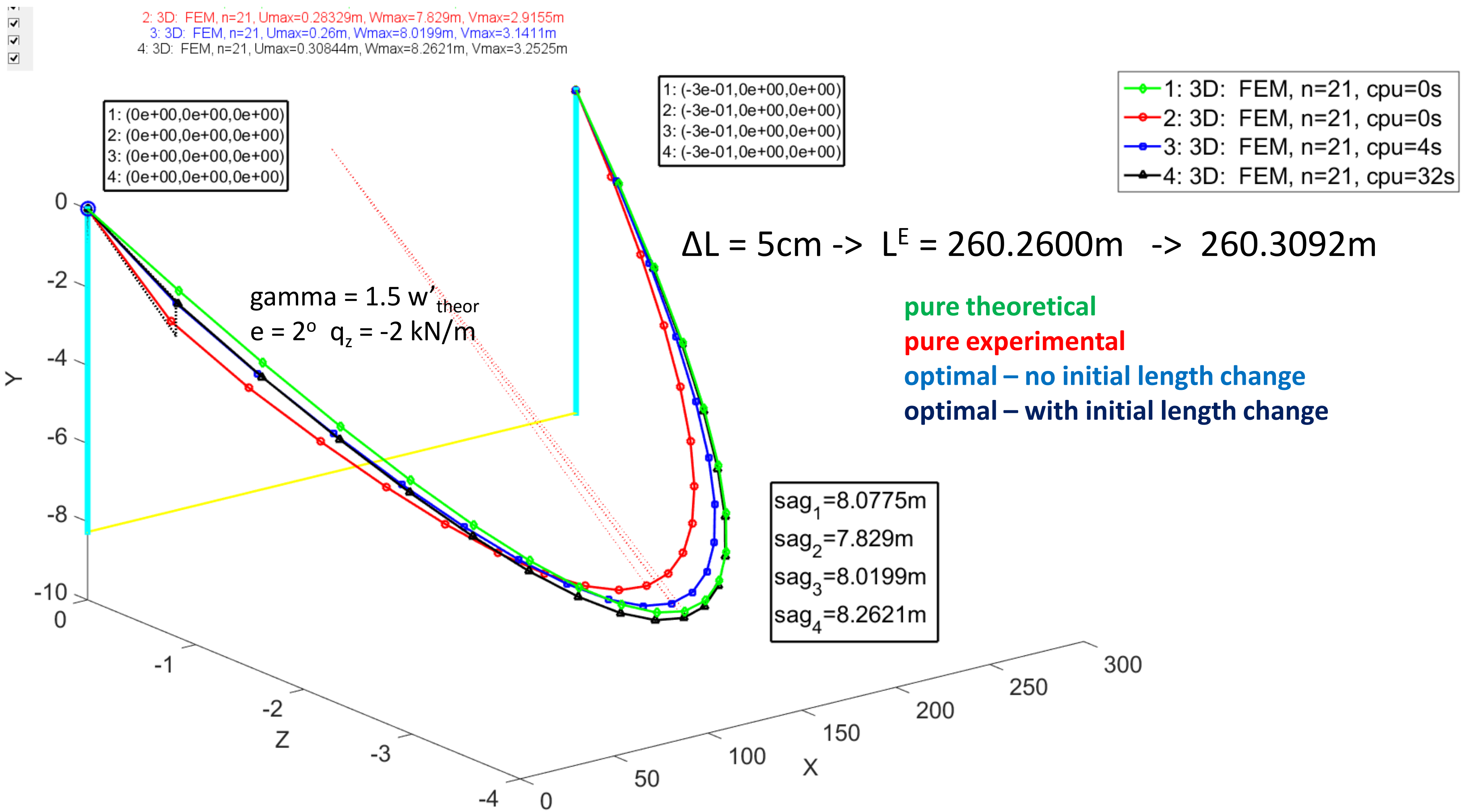

2: 3D: FEM, n=21, Umax=0.28329m, Wmax=7.829m, Vmax=2.9155m
3: 3D: FEM, n=21, Umax=0.26m, Wmax=8.0199m, Vmax=3.1411m
4: 3D: FEM, n=21, Umax=0.30844m, Wmax=8.2621m, Vmax=3.2525m
1: (0e+00,0e+00,0e+00)
2: (0e+00,0e+00,0e+00)
3: (0e+00,0e+00,0e+00)
4: (0e+00,0e+00,0e+00)
1: (-3e-01,0e+00,0e+00)
2: (-3e-01,0e+00,0e+00)
3: (-3e-01,0e+00,0e+00)
4: (-3e-01,0e+00,0e+00)
1: 3D: FEM, n=21, cpu=0s
2: 3D: FEM, n=21, cpu=0s
3: 3D: FEM, n=21, cpu=4s
4: 3D: FEM, n=21, cpu=32s
ΔL = 5cm -> L^E = 260.2600m -> 260.3092m
gamma = 1.5 w'theor
e = 2° qz = -2 kN/m
pure theoretical
pure experimental
optimal – no initial length change
optimal – with initial length change
sag1=8.0775m
sag2=7.829m
sag3=8.0199m
sag4=8.2621m
0
-2
-4
-6
-8
-10
Y
0
-1
-2
-3
-4
Z
0
50
100
150
200
250
300
X

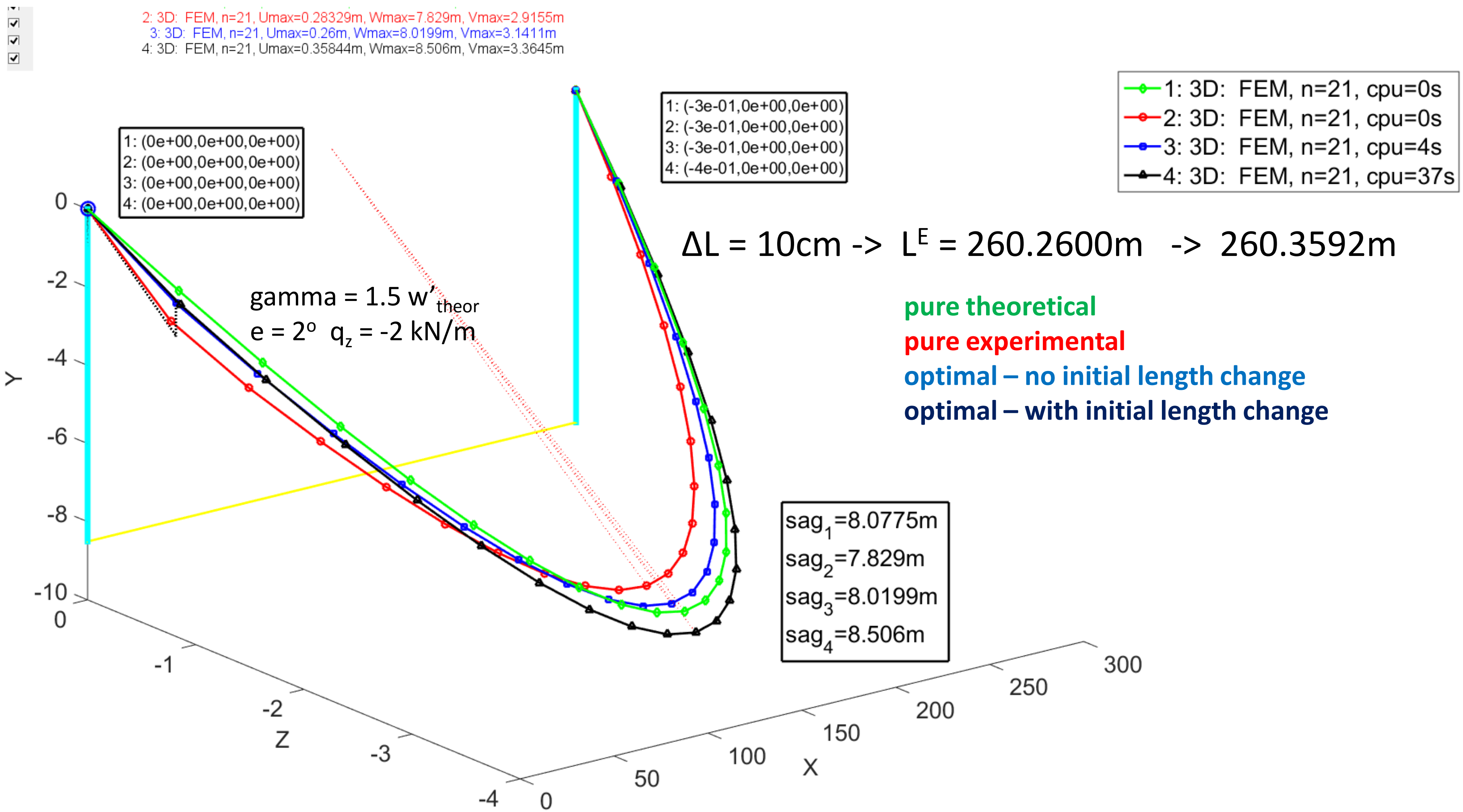

2: 3D: FEM, n=21, Umax=0.28329m, Wmax=7.829m, Vmax=2.9155m
3: 3D: FEM, n=21, Umax=0.26m, Wmax=8.0199m, Vmax=3.1411m
4: 3D: FEM, n=21, Umax=0.35844m, Wmax=8.506m, Vmax=3.3645m
1: 3D: FEM, n=21, cpu=0s
2: 3D: FEM, n=21, cpu=0s
3: 3D: FEM, n=21, cpu=4s
4: 3D: FEM, n=21, cpu=37s
1: (0e+00,0e+00,0e+00)
2: (0e+00,0e+00,0e+00)
3: (0e+00,0e+00,0e+00)
4: (0e+00,0e+00,0e+00)
1: (-3e-01,0e+00,0e+00)
2: (-3e-01,0e+00,0e+00)
3: (-3e-01,0e+00,0e+00)
4: (-4e-01,0e+00,0e+00)
ΔL = 10cm -> L^E = 260.2600m -> 260.3592m
gamma = 1.5 w'theor
e = 2° qz = -2 kN/m
pure theoretical
pure experimental
optimal – no initial length change
optimal – with initial length change
sag1=8.0775m
sag2=7.829m
sag3=8.0199m
sag4=8.506m
Y
Z
X

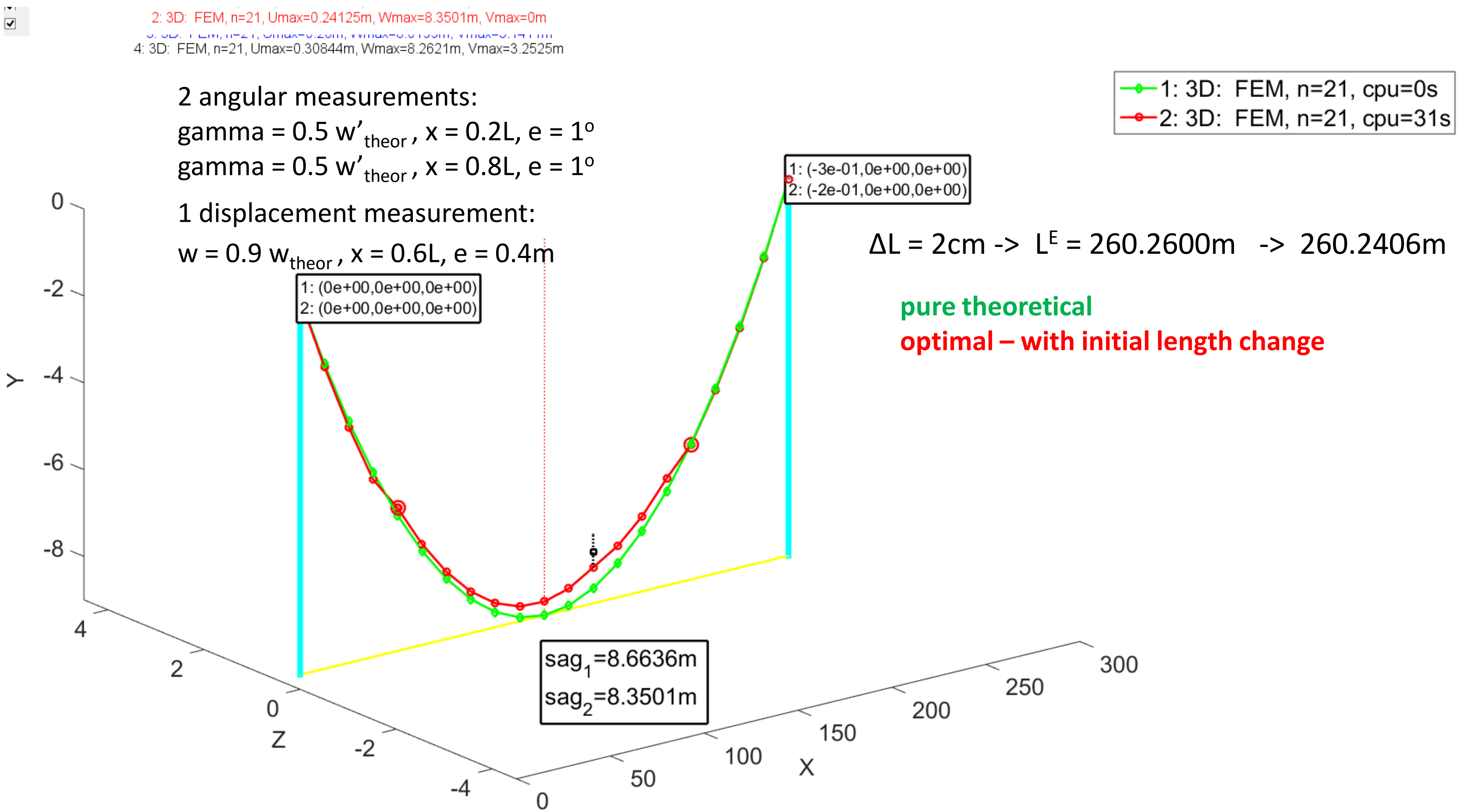

2: 3D: FEM, n=21, Umax=0.24125m, Wmax=8.3501m, Vmax=0m
4: 3D: FEM, n=21, Umax=0.30844m, Wmax=8.2621m, Vmax=3.2525m
2 angular measurements:
gamma = 0.5 w'theor , x = 0.2L, e = 1o
gamma = 0.5 w'theor , x = 0.8L, e = 1o
1 displacement measurement:
w = 0.9 wtheor , x = 0.6L, e = 0.4m
1: 3D: FEM, n=21, cpu=0s
2: 3D: FEM, n=21, cpu=31s
1: (-3e-01,0e+00,0e+00)
2: (-2e-01,0e+00,0e+00)
1: (0e+00,0e+00,0e+00)
2: (0e+00,0e+00,0e+00)
ΔL = 2cm -> LE = 260.2600m -> 260.2406m
pure theoretical
optimal – with initial length change
sag1=8.6636m
sag2=8.3501m
Y
Z
X
0
-2
-4
-6
-8
4
2
0
-2
-4
0
50
100
150
200
250
300

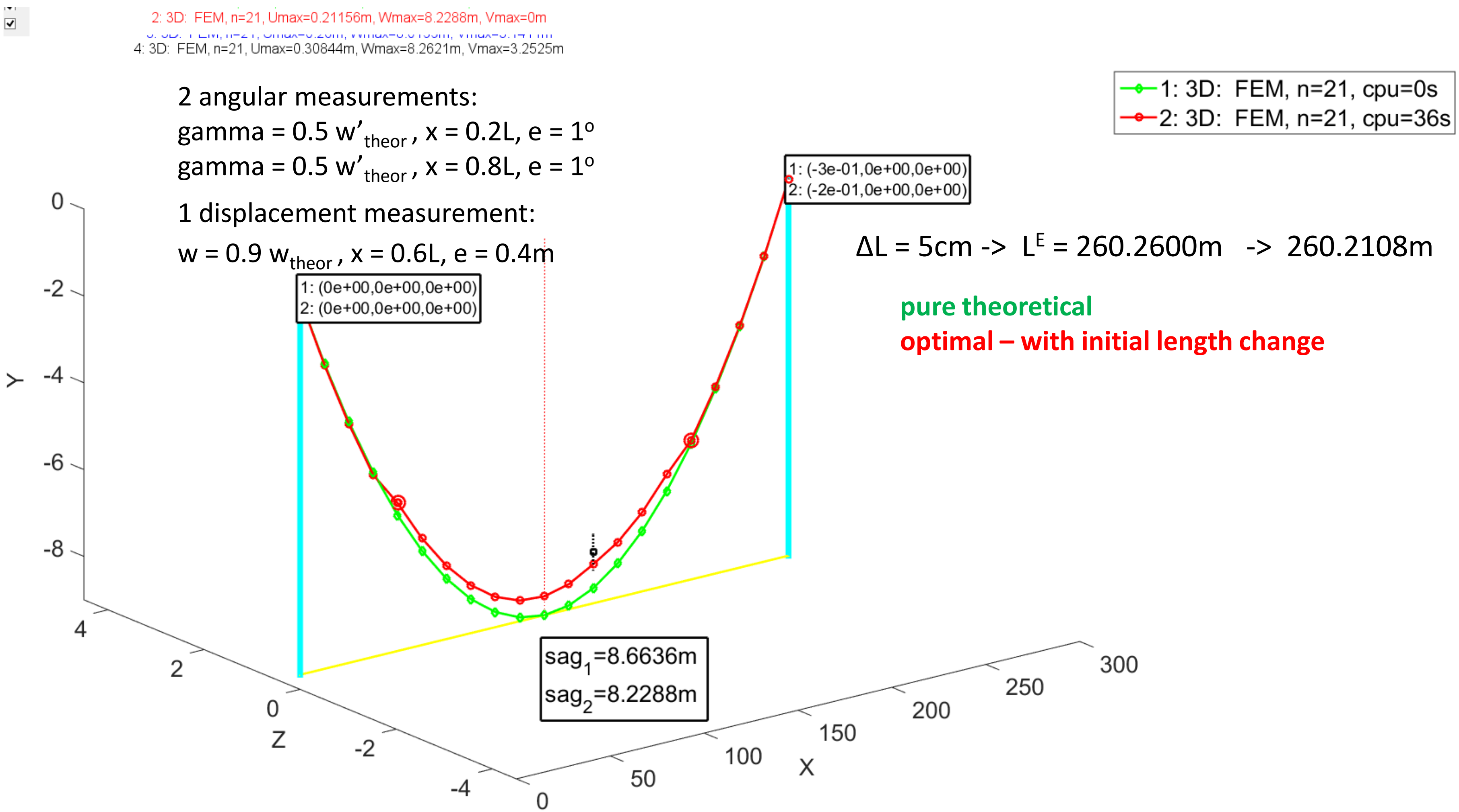
2: 3D: FEM, n=21, Umax=0.21156m, Wmax=8.2288m, Vmax=0m
4: 3D: FEM, n=21, Umax=0.30844m, Wmax=8.2621m, Vmax=3.2525m
2 angular measurements:
gamma = 0.5 w'_{theor} , x = 0.2L, e = 1°
gamma = 0.5 w'_{theor} , x = 0.8L, e = 1°
1 displacement measurement:
w = 0.9 w_{theor} , x = 0.6L, e = 0.4m
1: 3D: FEM, n=21, cpu=0s
2: 3D: FEM, n=21, cpu=36s
1: (-3e-01,0e+00,0e+00)
2: (-2e-01,0e+00,0e+00)
1: (0e+00,0e+00,0e+00)
2: (0e+00,0e+00,0e+00)
ΔL = 5cm -> L^E = 260.2600m -> 260.2108m
pure theoretical
optimal – with initial length change
sag_1=8.6636m
sag_2=8.2288m
Y
0
-2
-4
-6
-8
Z
4
2
0
-2
-4
X
0
50
100
150
200
250
300

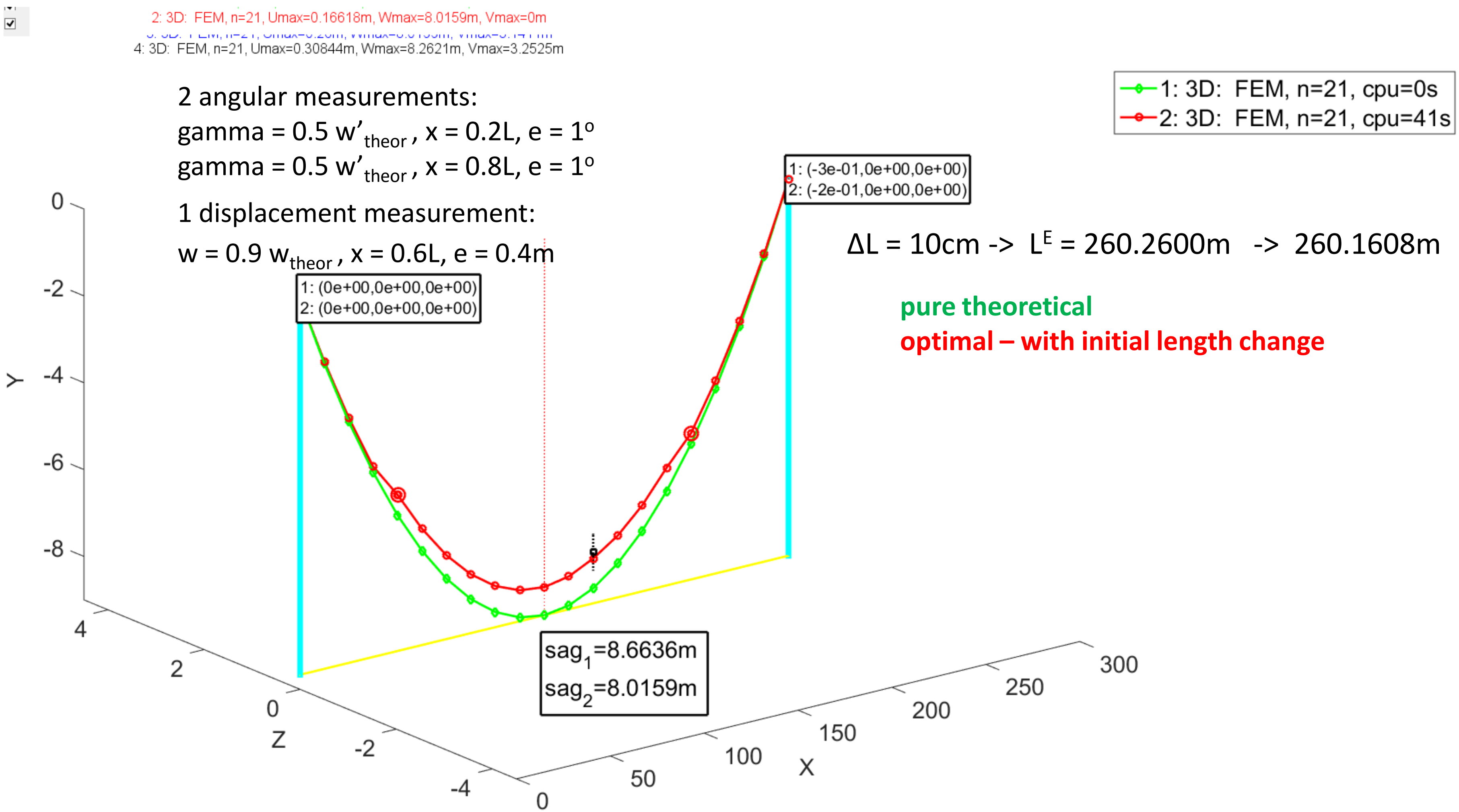

2: 3D: FEM, n=21, Umax=0.16618m, Wmax=8.0159m, Vmax=0m
4: 3D: FEM, n=21, Umax=0.30844m, Wmax=8.2621m, Vmax=3.2525m
2 angular measurements:
gamma = 0.5 w'theor , x = 0.2L, e = 1°
gamma = 0.5 w'theor , x = 0.8L, e = 1°
1 displacement measurement:
w = 0.9 wtheor , x = 0.6L, e = 0.4m
1: 3D: FEM, n=21, cpu=0s
2: 3D: FEM, n=21, cpu=41s
1: (-3e-01,0e+00,0e+00)
2: (-2e-01,0e+00,0e+00)
1: (0e+00,0e+00,0e+00)
2: (0e+00,0e+00,0e+00)
ΔL = 10cm -> L^E = 260.2600m -> 260.1608m
pure theoretical
optimal – with initial length change
sag1=8.6636m
sag2=8.0159m
Y
0
-2
-4
-6
-8
Z
4
2
0
-2
-4
X
0
50
100
150
200
250
300

PILOT ANALYSIS FOR TAURON POWER TRANSMISSION LINE

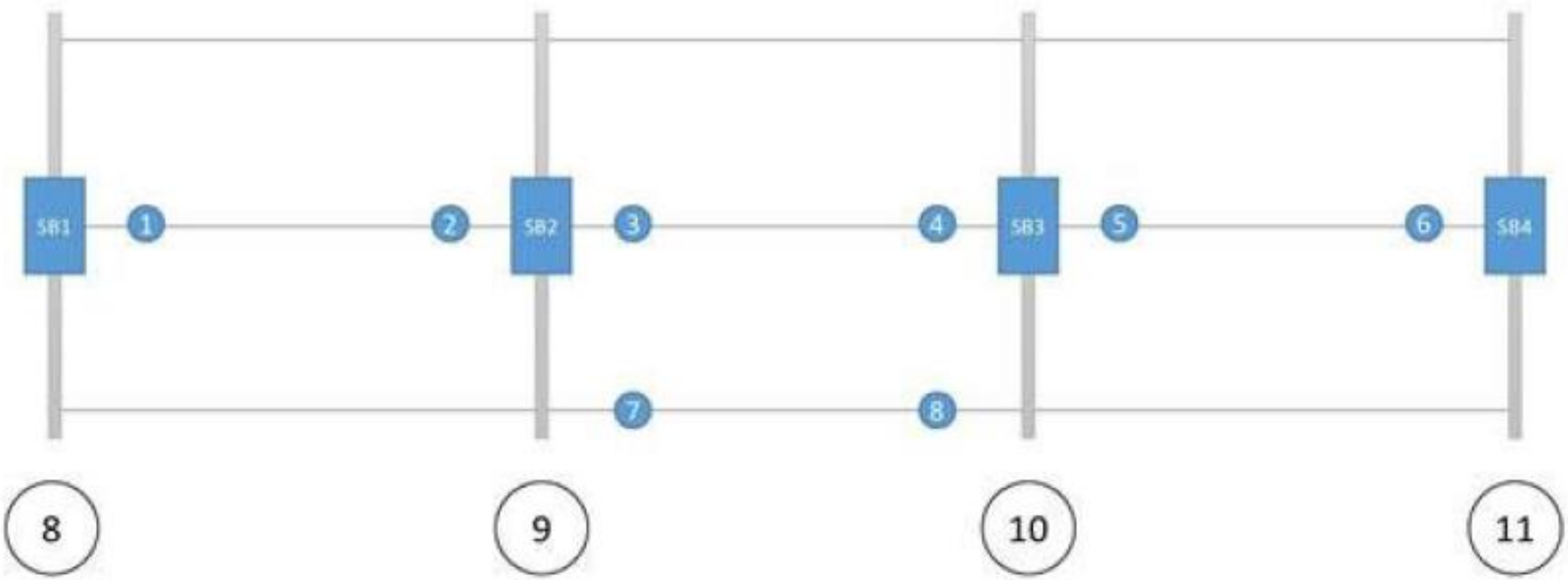

base station tower mounted

tower

cable registration device

conductors

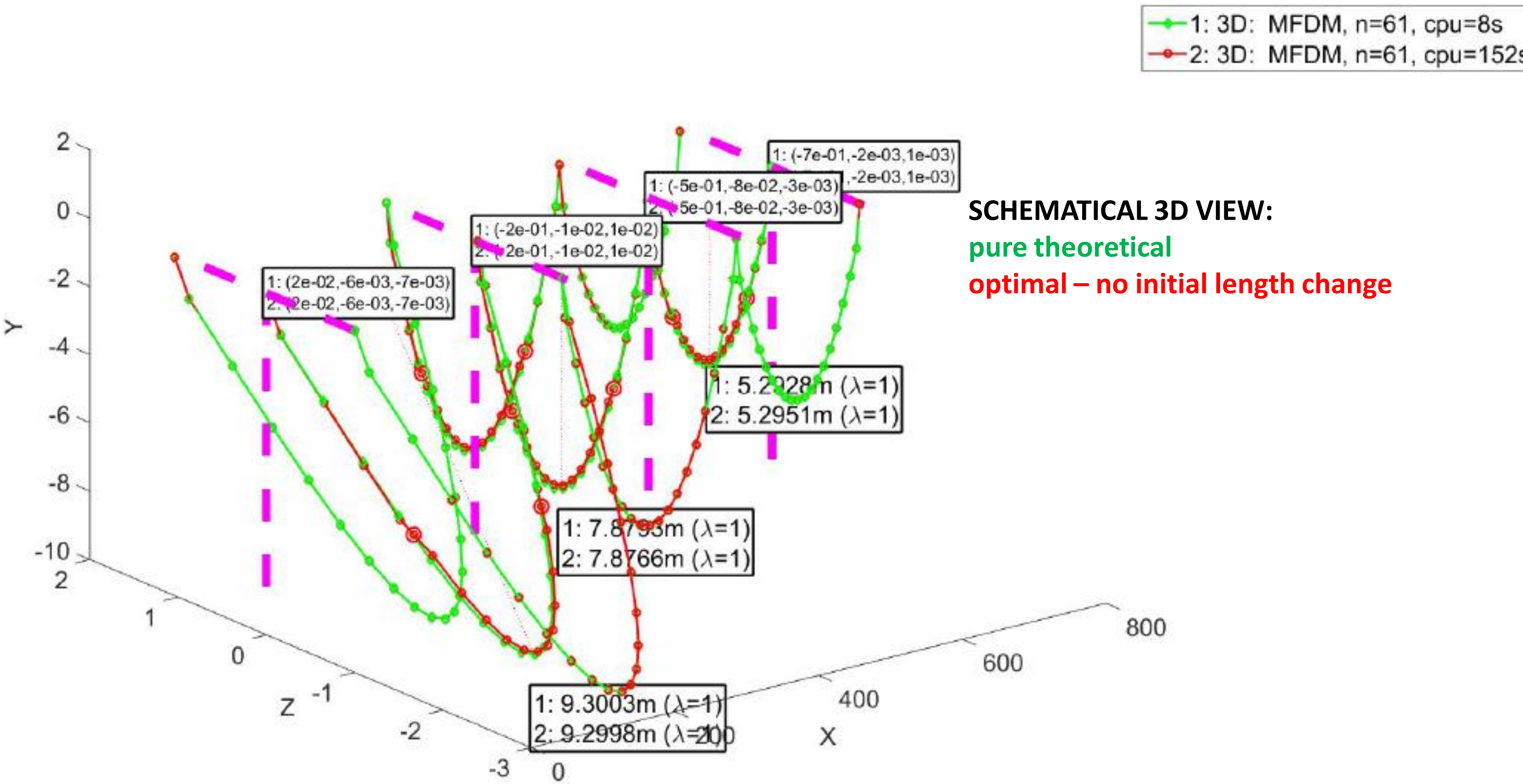

SCHEMATICAL 3D VIEW:

pure theoretical

optimal – no initial length change

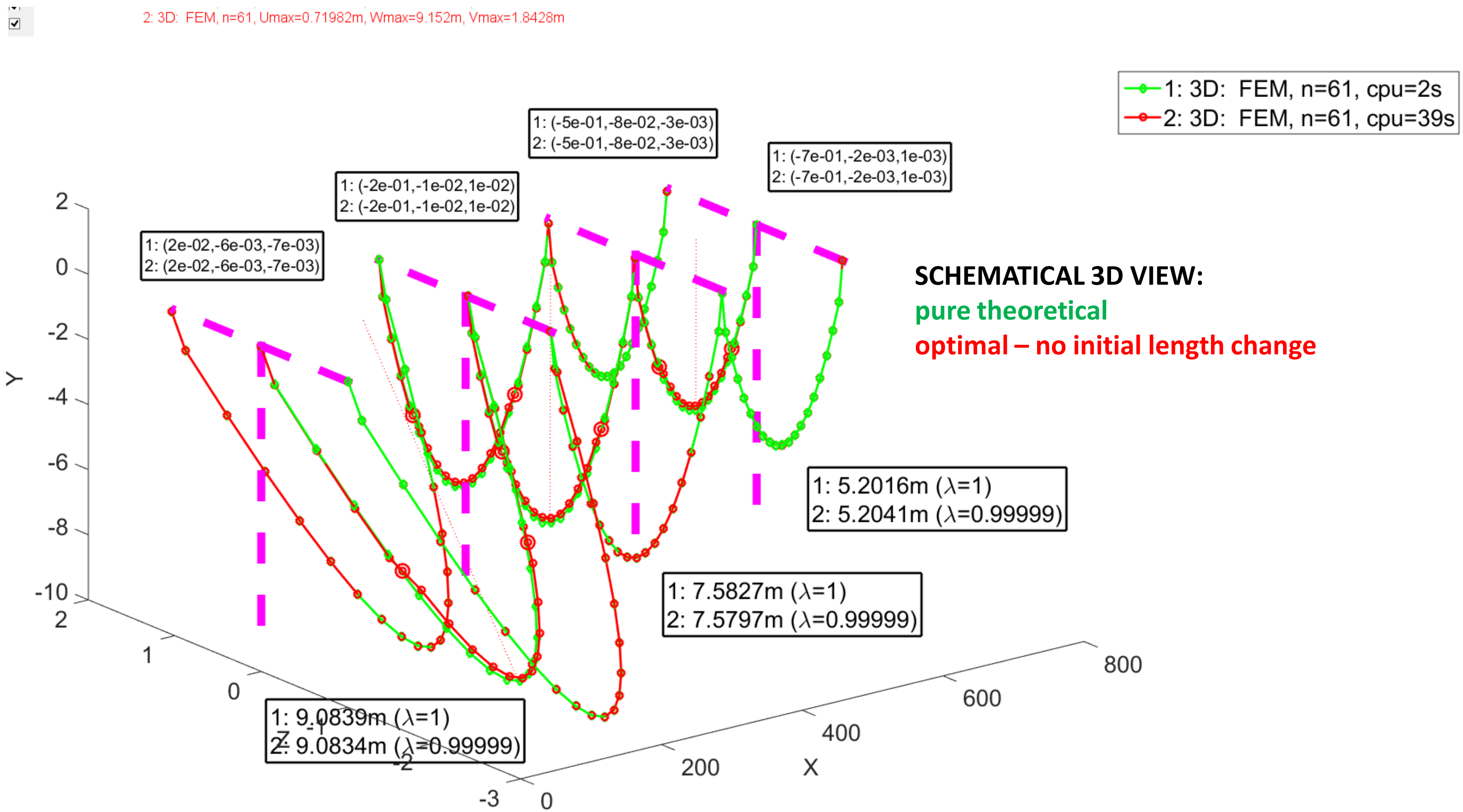

2: 3D: FEM, n=61, Umax=0.71982m, Wmax=9.152m, Vmax=1.8428m
1: 3D: FEM, n=61, cpu=2s
2: 3D: FEM, n=61, cpu=39s
1: (2e-02,-6e-03,-7e-03)
2: (2e-02,-6e-03,-7e-03)
1: (-2e-01,-1e-02,1e-02)
2: (-2e-01,-1e-02,1e-02)
1: (-5e-01,-8e-02,-3e-03)
2: (-5e-01,-8e-02,-3e-03)
1: (-7e-01,-2e-03,1e-03)
2: (-7e-01,-2e-03,1e-03)
SCHEMATICAL 3D VIEW:
pure theoretical
optimal – no initial length change
1: 5.2016m (λ=1)
2: 5.2041m (λ=0.99999)
1: 7.5827m (λ=1)
2: 7.5797m (λ=0.99999)
1: 9.0839m (λ=1)
2: 9.0834m (λ=0.99999)
Y
X
Z

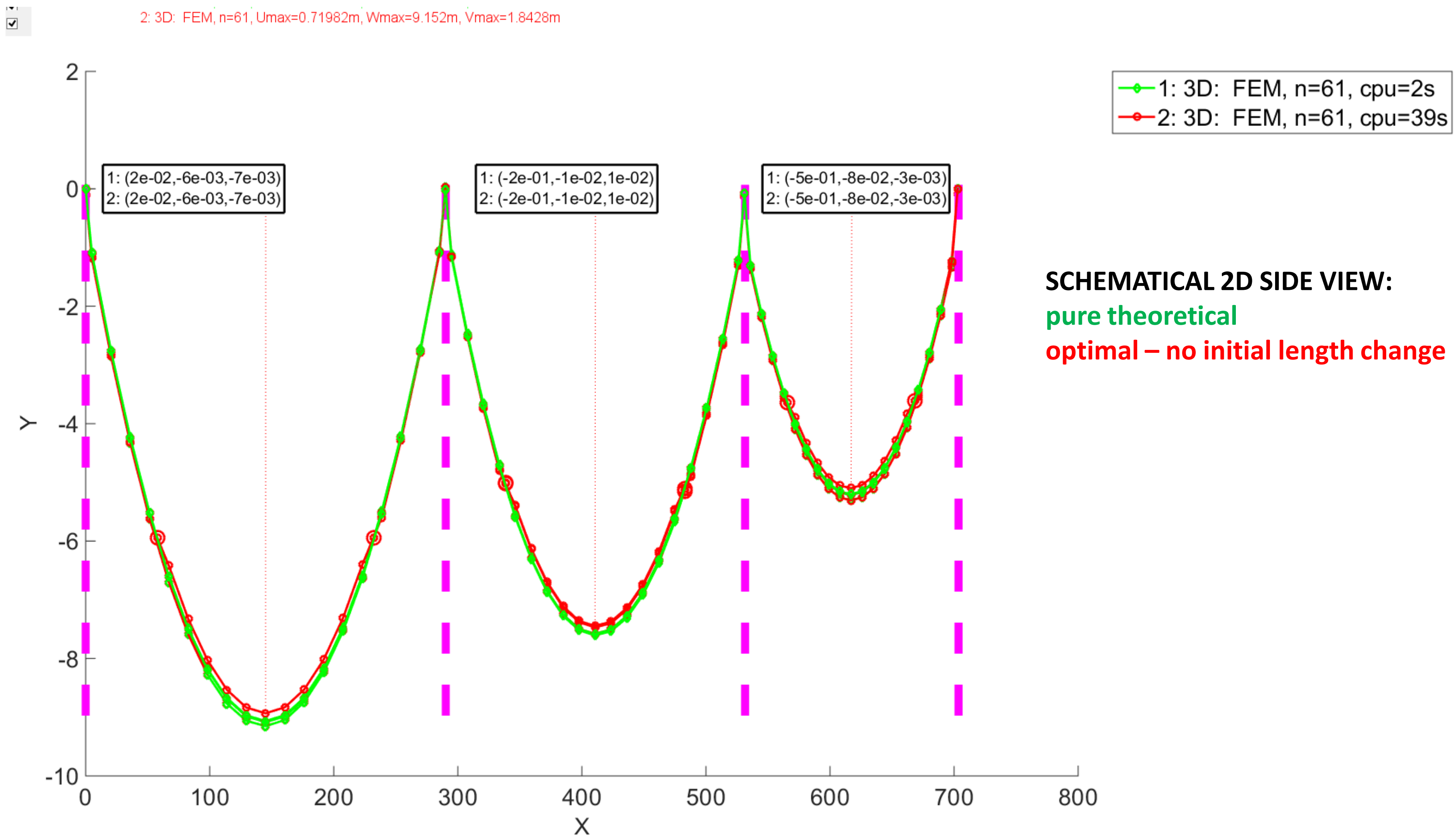

SCHEMATICAL 2D SIDE VIEW:

pure theoretical

optimal – no initial length change

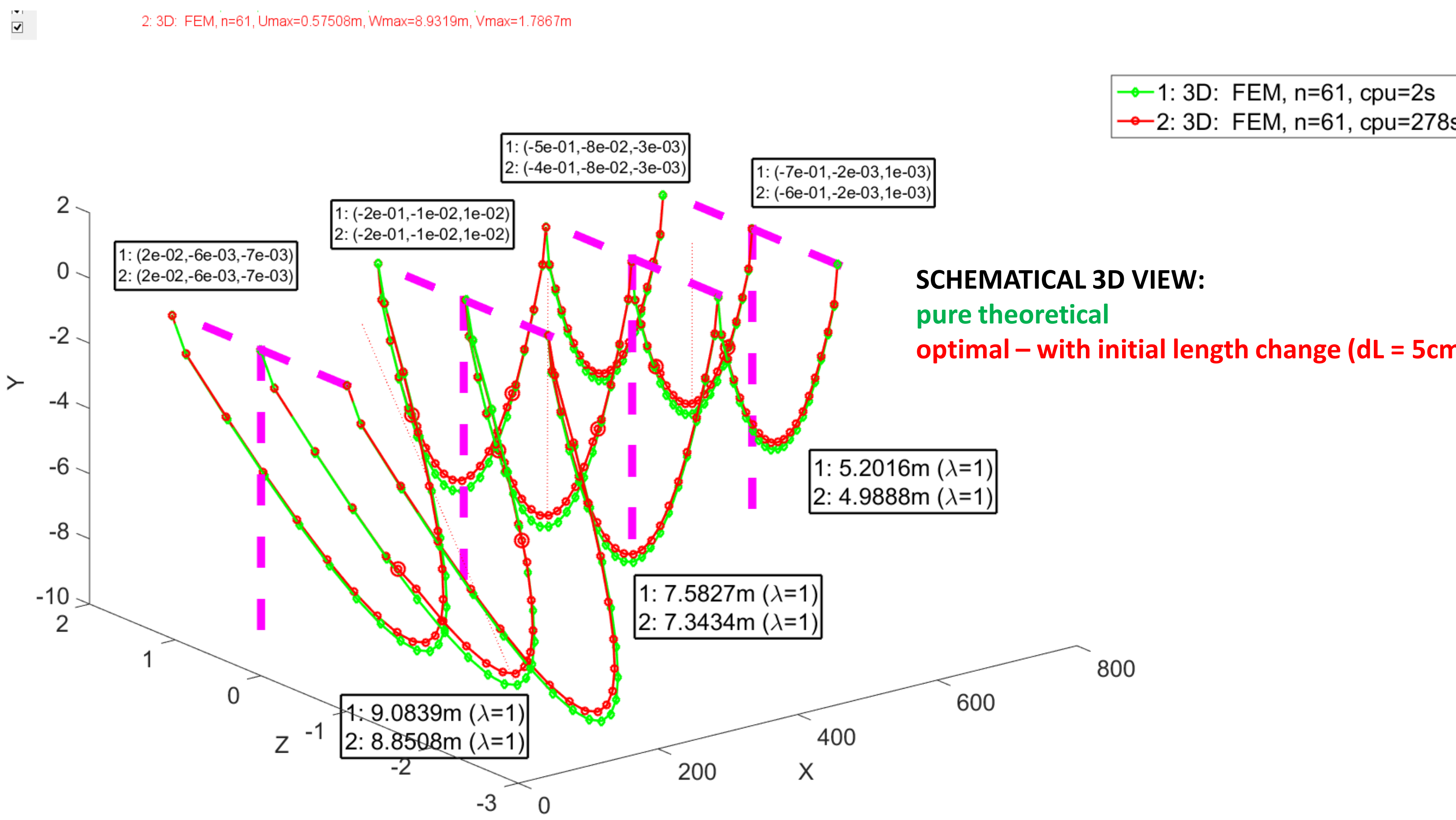

SCHEMATICAL 3D VIEW:

pure theoretical

optimal – with initial length change (dL = 5cm)

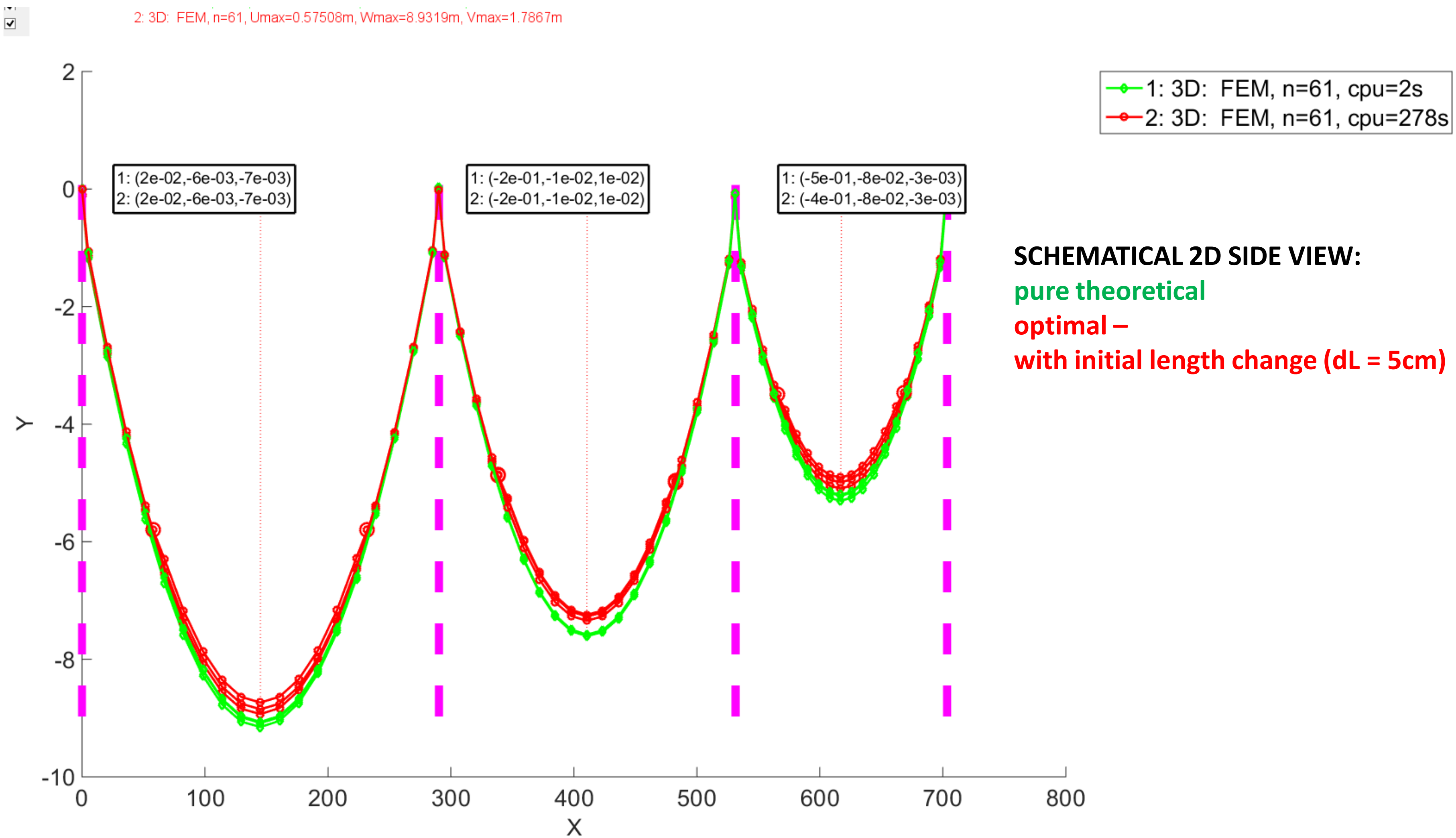

SCHEMATICAL 2D SIDE VIEW:

pure theoretical

optimal –

with initial length change (dL = 5cm)

PILOT STEERING CODE

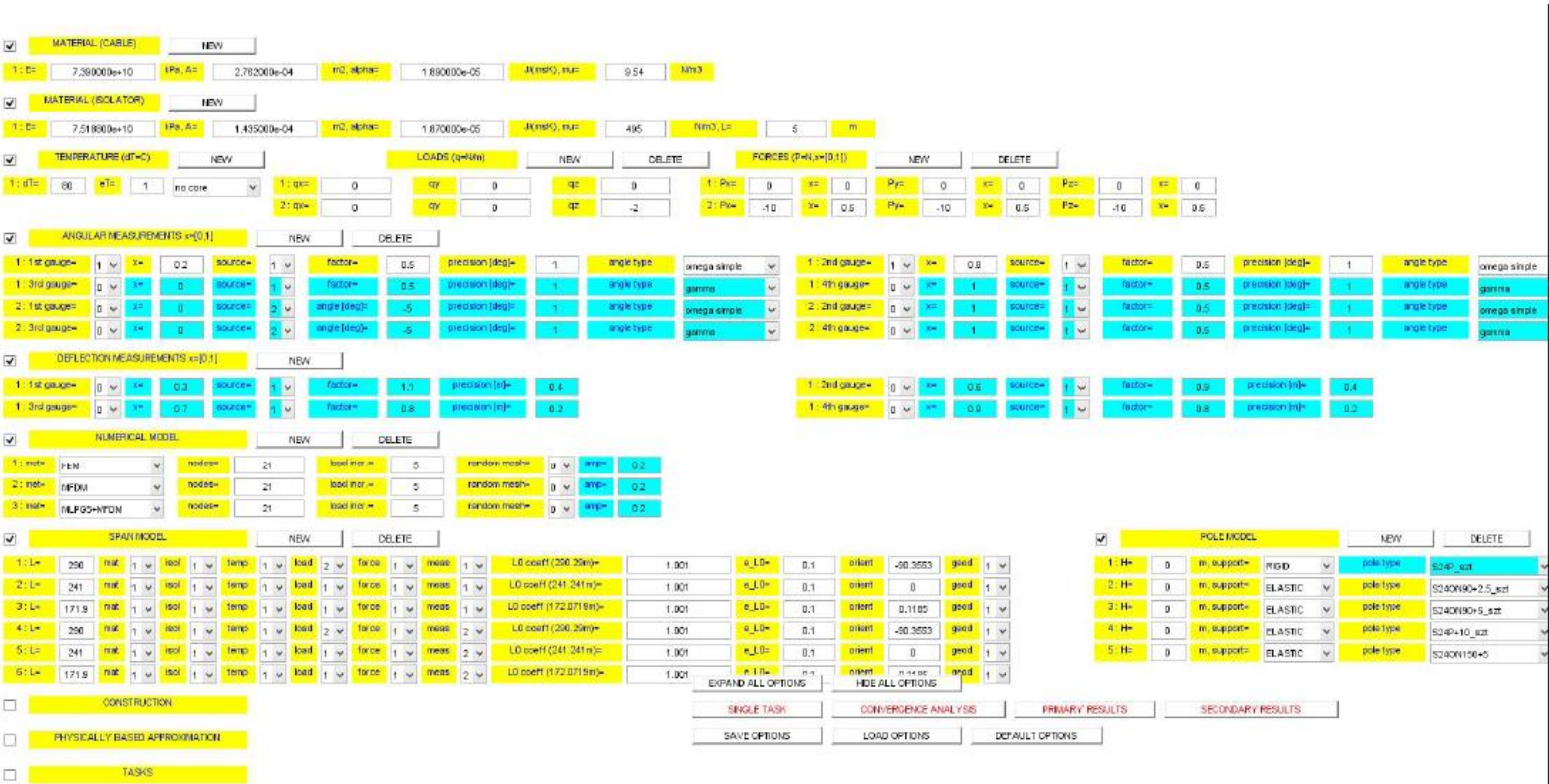

6. Final remarks

6.1 Brief summary

- **Developed** and preliminary **tested** were reliable mechanical and mathematical models as well as relevant study computer codes providing very fast and precise **3D analysis** of **large cable** displacements, as well as 3 spans sections of **overhead power transmission** lines.

- Due to real engineering problem considered special attention was paid to **reliability** of the results obtained. Therefore, several independent approaches were investigated including

  = series of 1D, 2D, and 3D **models**

  = strong, weak and hybrid mixed **formulations**

  = several **methods** of discrete analysis (FEM, MFDM, MFDM + MLPG)

  = various **orders** of approximation

  = three different computer **codes** (two ours)

  = various methods of **non-linear** analysis

- For these approaches examined and compared were

  = **precision** of results obtained (a-posteriori error analysis), their

  = **convergence**, and convergence rate

  = **stability**

  = **efficiency** (computational time)

- Results of **innovative on-line measurements** (weather data and cable inclination and rotation angles) were incorporated into analysis of large displacements of cables. **Two** different solution **approaches** are proposed

  = **simultaneous hybrid** analysis using the **theory** of mechanics and **all on-line measurements** was considered within the Physically Based Approximation (**PBA**) solution approach. However, such PBA application required its modification, namely **extension** of the original method onto its **new variational formulation**.

  = search for the optimal set of measured data minimizing descripancy between calculated and measured quantities. New b.v.p. solution for such data is found then.

- The **original** elements of this research include:

  = **innovative** problem formulation

  = **exact analytical 3D** solution of cable b.v. problem

  = **first MFDM** application to overhead power lines

  = **comparison** of various solution approaches

- The solution approach developed here is carried out for the benefit of **real engineering** problem of **dynamic management** of overhead power lines.

- The existing policy of **dichotomous** summer and winter **safety** thresholds, limiting power transmission may be replaced by **dynamic** management based on innovative on-line measurements, and analysis provided by our research reported here. Such policy would allow for more **efficient** use of **existing** overhead power transmission lines.

6.2 Future investigations

- All tests, performed so far, used **simulated** experimental data; application of the true measured data is planned now.
- However, a **calibration** of the models of overhead power lines developed here is required first; it is based on the true conductors **configuration** data occasionally obtained by means of **surveying.**
- After calibration, the final **verification** and **validation** of the models developed in this research may be done; finally one may use them in **real engineering** analysis of the type **I, II or III** earlier defined.

THANK YOU VERY MUCH FOR ATTENTION

2: 3D: FEM, n=121, Umax=0.71986m, Wmax=9.1452m, Vmax=1.8211m

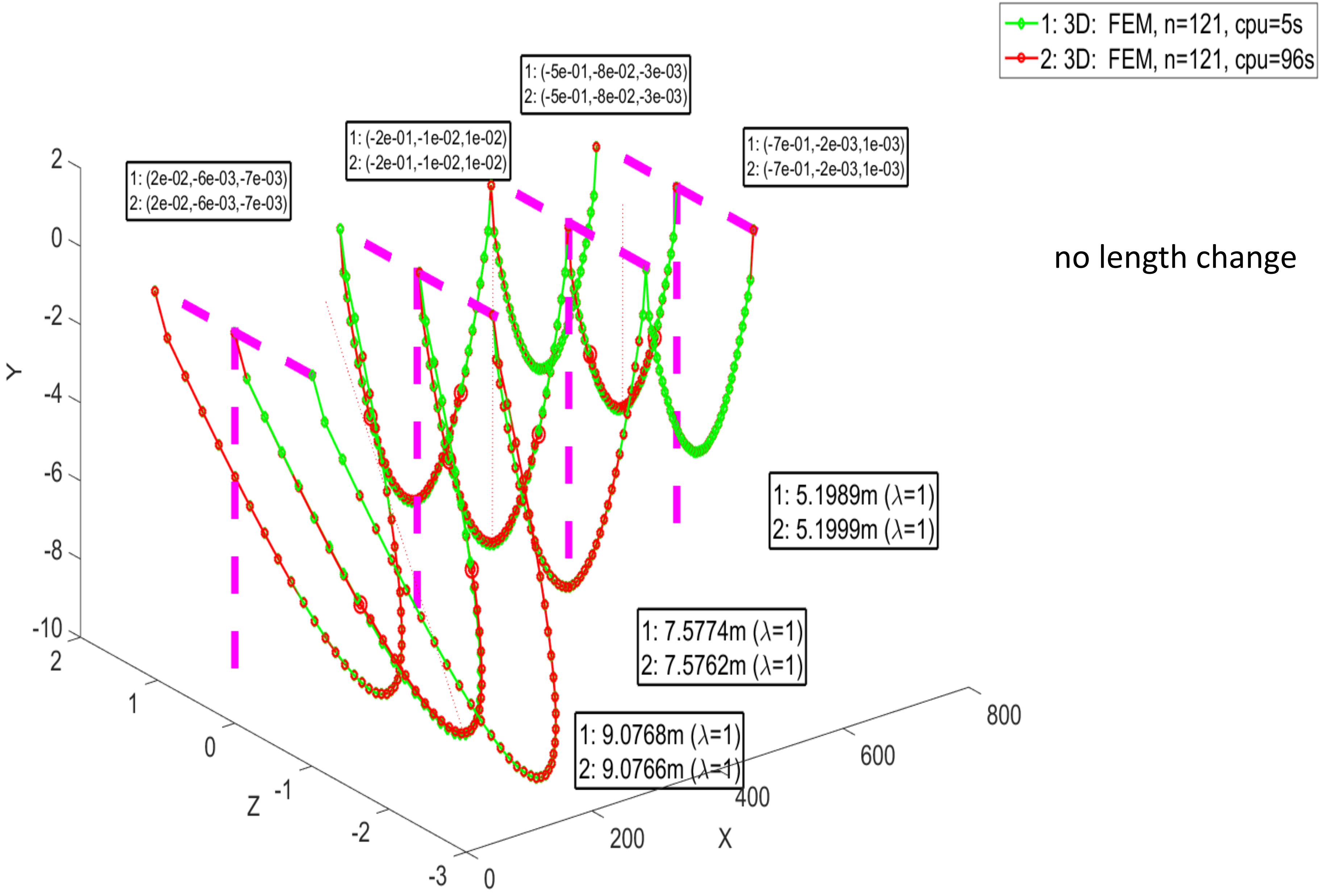

no length change

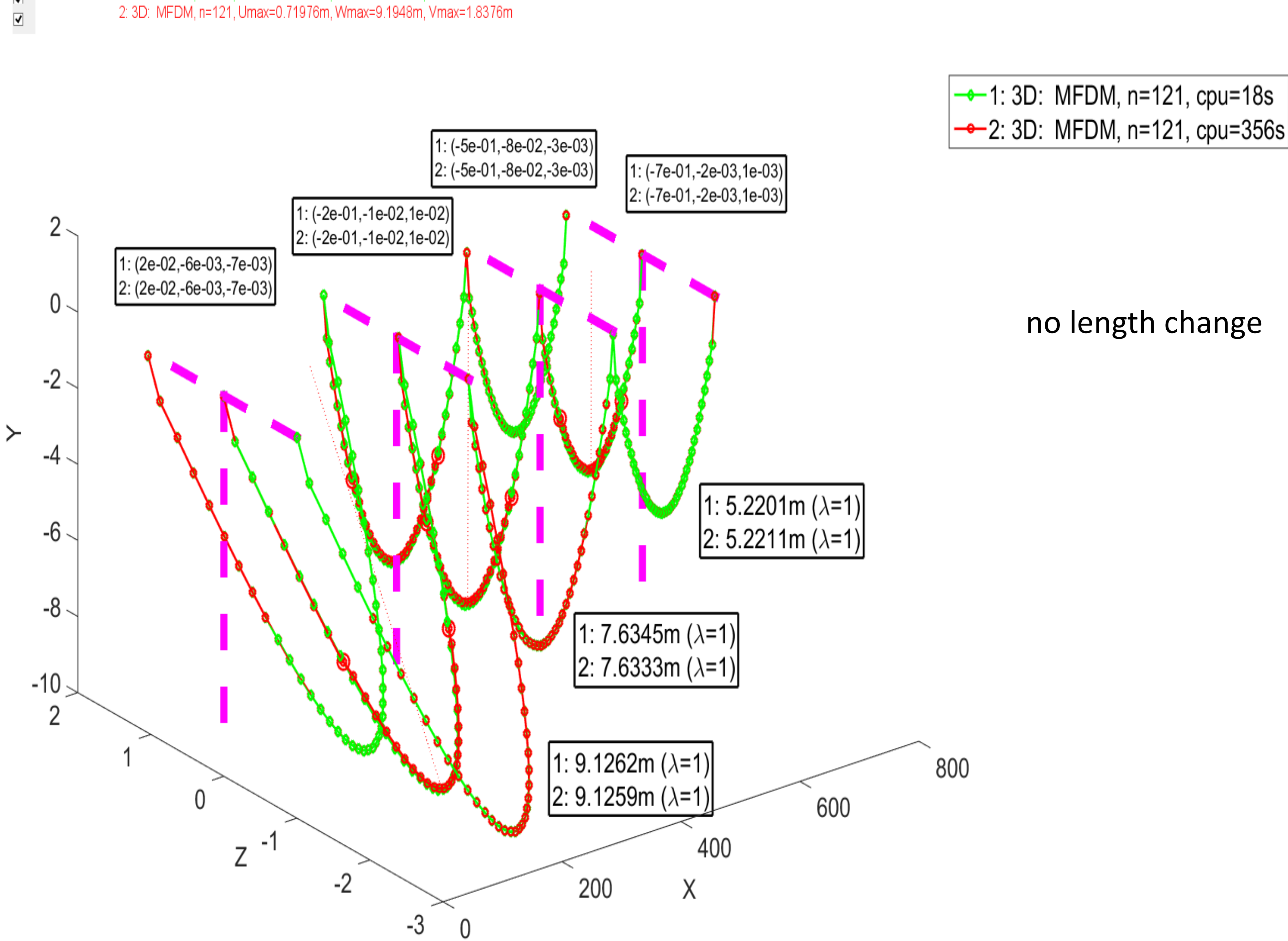

no length change

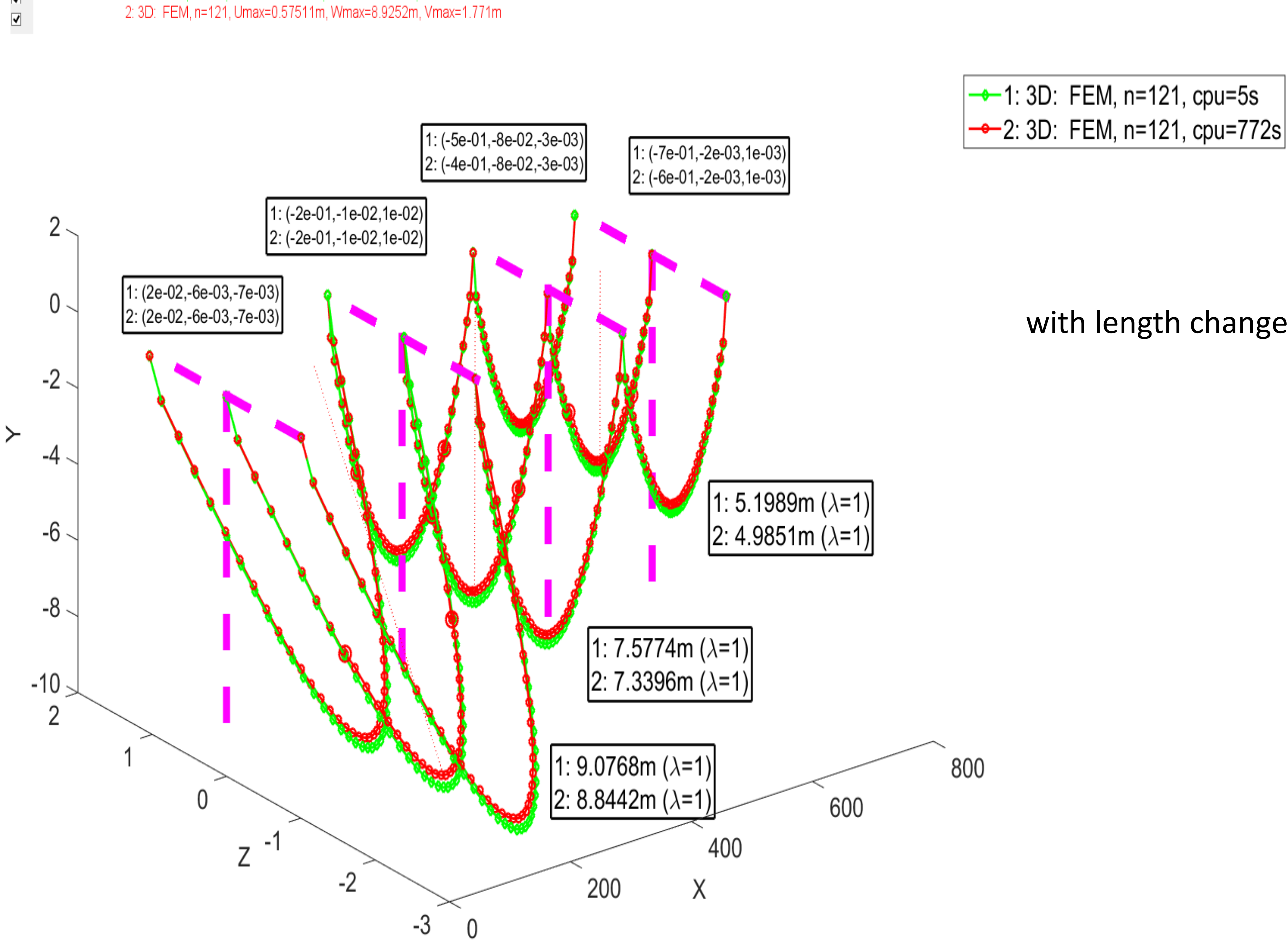

with length change

2: 3D: MFDM, n=121, Umax=0.575m, Wmax=8.9726m, Vmax=1.787m

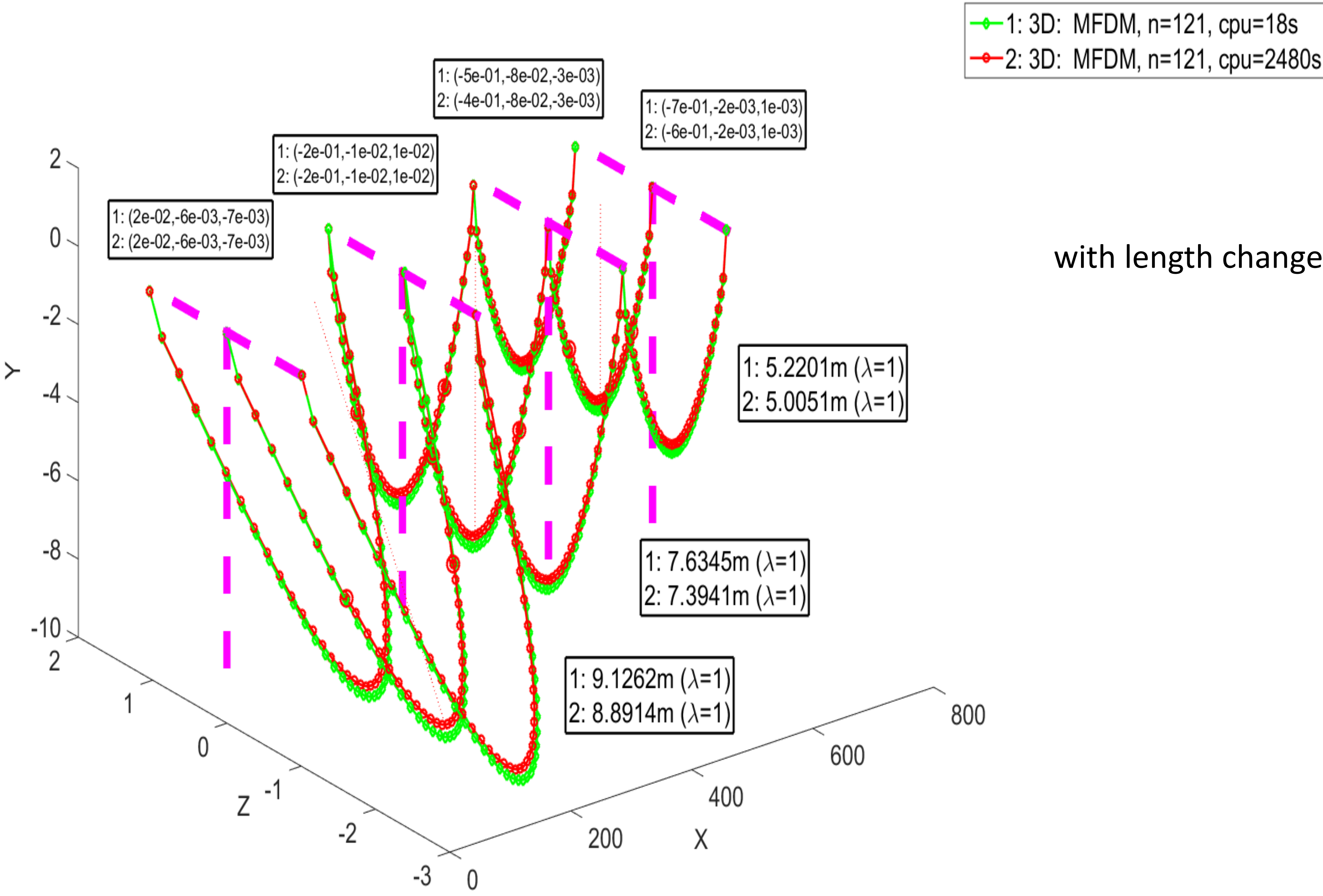

with length change

EKSPERYMENTALNIE WSPOMAGANE OSZACOWANIE BEZPIECZNEJ SKRAJNI LINII ENERGETYCZNYCH WYSOKICH NAPIĘĆ

1. WSTĘP

1.1 Problematyka badań

Dziś będzie mowa o **przesyłaniu** energii elektrycznej.

Wszyscy potrzebujemy tej energii. Czy są **zagrożenia** w jej przesyłaniu?

kłopoty	-	**limity** przesyłu - stopnie zasilania
realia	-	przestarzała (40 lat) infrastruktura linii elektroenergetycznych
	-	dopuszczalne jedynie **2** progi: lato (upał) i zima (lód)
propozycja	-	**S**ystem **D**ynamicznego **Z**arządzania **P**rzesyłem przy wykorzystaniu innowacyjnych pomiarów on-line; rola operatora
efekty	-	zysk: SDZP < 15% **grafen** (alternatywa) 100% ÷ 200%
konsorcjum	-	Uczelnie 5, PAN, Firmy 2, Operatorzy sieci 3
sponsor	-	GEKON (**Ge**nerator **Kon**cepcji Ekologicznych) Program: 1) Narodowy Fundusz Ochrony Środowiska i Gospodarki Wodnej 2) Narodowe Centrum Badań i Rozwoju

Data characteristics

1. **Technical** data
   - **supporting** structures
   - chains of **insulators**
   - **conductors**
   - **in-situ** characteristics (e.g. shape of various obstacles)

2. **Measured** data
   - **measurement** location
     - data collector and sensor (BS) – on supporting structure
     - sensor (R) – on conductors
   - weather and electric current data
   - conductor inclination and location data
   - calibration and validation data (initial line status)

   on-line measurement frequency – 10 min

3. **Weather forecast** 6-72 h (**I**nstitute of **C**omputational **M**athematics) and electric current data (network operators)

3.10 **Stiffness** matrices and **loading** vectors for both the **FEM** and **MFD** methods

$$\left(\boldsymbol{K}_T{}^{(e)}\right)^{(k)} = \int_0^h \begin{bmatrix} \boldsymbol{B}_{v_1}^{(e)} \\ \boldsymbol{B}_{v_2}^{(e)} \\ \boldsymbol{B}_{v_3}^{(e)} \end{bmatrix}^t \begin{bmatrix} \left(\Delta F_{1,1}{}^{(e)}\right)^{(k)} \boldsymbol{B}_{\psi_1}^{(e)} + \left(\Delta F_{1,2}{}^{(e)}\right)^{(k)} \boldsymbol{B}_{\psi_2}^{(e)} + \left(\Delta F_{1,3}{}^{(e)}\right)^{(k)} \boldsymbol{B}_{\psi_3}^{(e)} \\ \left(\Delta F_{2,1}{}^{(e)}\right)^{(k)} \boldsymbol{B}_{\psi_1}^{(e)} + \left(\Delta F_{2,2}{}^{(e)}\right)^{(k)} \boldsymbol{B}_{\psi_2}^{(e)} + \left(\Delta F_{2,3}{}^{(e)}\right)^{(k)} \boldsymbol{B}_{\psi_3}^{(e)} \\ \left(\Delta F_{3,1}{}^{(e)}\right)^{(k)} \boldsymbol{B}_{\psi_1}^{(e)} + \left(\Delta F_{3,2}{}^{(e)}\right)^{(k)} \boldsymbol{B}_{\psi_2}^{(e)} + \left(\Delta F_{3,3}{}^{(e)}\right)^{(k)} \boldsymbol{B}_{\psi_3}^{(e)} \end{bmatrix} dX +$$

$$- h\int_0^h \begin{bmatrix} \boldsymbol{N}_{v_1}^{(e)} \\ \boldsymbol{N}_{v_2}^{(e)} \\ \boldsymbol{N}_{v_3}^{(e)} \end{bmatrix}^t \begin{bmatrix} \left(\Delta p_{1,1}{}^{(e)}\right)^{(k)} \boldsymbol{B}_{\psi_1}^{(e)} + \left(\Delta p_{1,2}{}^{(e)}\right)^{(k)} \boldsymbol{B}_{\psi_2}^{(e)} + \left(\Delta p_{1,3}{}^{(e)}\right)^{(k)} \boldsymbol{B}_{\psi_3}^{(e)} \\ \left(\Delta p_{2,1}{}^{(e)}\right)^{(k)} \boldsymbol{B}_{\psi_1}^{(e)} + \left(\Delta p_{2,2}{}^{(e)}\right)^{(k)} \boldsymbol{B}_{\psi_2}^{(e)} + \left(\Delta p_{2,3}{}^{(e)}\right)^{(k)} \boldsymbol{B}_{\psi_3}^{(e)} \\ \left(\Delta p_{3,1}{}^{(e)}\right)^{(k)} \boldsymbol{B}_{\psi_1}^{(e)} + \left(\Delta p_{3,2}{}^{(e)}\right)^{(k)} \boldsymbol{B}_{\psi_2}^{(e)} + \left(\Delta p_{3,3}{}^{(e)}\right)^{(k)} \boldsymbol{B}_{\psi_3}^{(e)} \end{bmatrix} dX$$

$$\left(\boldsymbol{P}^{(e)}\right)^{(k)} = \int_0^h \begin{bmatrix} \boldsymbol{B}_{v_1}^{(e)} \\ \boldsymbol{B}_{v_2}^{(e)} \\ \boldsymbol{B}_{v_3}^{(e)} \end{bmatrix}^t \begin{bmatrix} \left(F_1^{(e)}\right)^{(k)} \\ \left(F_2^{(e)}\right)^{(k)} \\ \left(F_3^{(e)}\right)^{(k)} \end{bmatrix} dX - \int_0^h \begin{bmatrix} \boldsymbol{N}_{v_1}^{(e)} \\ \boldsymbol{N}_{v_2}^{(e)} \\ \boldsymbol{N}_{v_3}^{(e)} \end{bmatrix}^t \begin{bmatrix} \left(p_1^{(e)}\right)^{(k)} \\ \left(p_2^{(e)}\right)^{(k)} \\ \left(p_3^{(e)}\right)^{(k)} \end{bmatrix} dX$$

N – shape functions (MES, BMRS)

B – derivatives of shape functions

$$\boldsymbol{B}^{(e)} = \frac{d}{dX}\boldsymbol{N}^{(e)}$$